

A_4 modular invariance and the strong CP problem

S. T. Petcov ^{1,2*} and M. Tanimoto ³

¹*INFN/SISSA, Via Bonomea 265, 34136 Trieste, Italy*

²*Kavli IPMU (WPI), UTIAS, The University of Tokyo, Kashiwa, Chiba 277-8583, Japan*

³*Department of Physics, Niigata University, Ikarashi 2, Niigata 950-2181, Japan*

Abstract

We present simple effective theory of quark masses, mixing and CP violation with level $N = 3$ (A_4) modular symmetry, which provides solution to the strong CP problem without the need for an axion. The vanishing of the strong CP-violating phase $\bar{\theta}$ is ensured by assuming CP to be a fundamental symmetry of the Lagrangian of the theory. The CP symmetry is broken spontaneously by the vacuum expectation value (VEV) of the modulus τ . This provides the requisite large value of the CKM CP-violating phase while the strong CP phase $\bar{\theta}$ remains zero or is tiny. Within the considered framework we discuss phenomenologically viable quark mass matrices with three types of texture zeros, which are realized by assigning both the left-handed and right-handed quark fields to A_4 singlets $\mathbf{1}$, $\mathbf{1}'$ and $\mathbf{1}''$ with appropriate weights. The VEV of τ is restricted to reproduce the observed CKM parameters. We discuss cases in which the modulus VEV is close to the fixed points i , ω and $i\infty$. In particular, we focus on the VEV of τ , which gives the absolute minima of the supergravity-motivated modular- and CP-invariant potentials for the modulus τ , so called, modulus stabilisation. We present a successful model, which is consistent with the modulus stabilisation close to $\tau = \omega$.

*Also at: Institute of Nuclear Research and Nuclear Energy, Bulgarian Academy of Sciences, 1784 Sofia, Bulgaria.

1 Introduction

The strong CP problem has been a puzzle in particle physics since the QCD Lagrangian violates CP due to instanton effects [1–4]. The CP violation in QCD is described by the strong CP phase

$$\bar{\theta} = \theta_{\text{QCD}} + \arg \det [M_U M_D], \quad (1)$$

where M_U and M_D denote the mass matrices of the up-type and the down-type quarks, respectively, and θ_{QCD} is the coefficient of the topological charge term in the QCD Lagrangian:

$$\mathcal{L}_{\text{QCD}} = \bar{Q}(i \not{D} - M_Q)Q - \frac{1}{4} \text{Tr} G^2 + \theta_{\text{QCD}} \frac{g_3^2}{32\pi^2} \text{Tr} G\tilde{G}. \quad (2)$$

Here G is the gluon field stress tensor and Q is the multiplet of quark fields with definite masses. While θ_{QCD} and $\arg \det [M_U M_D]$ are transformed into each other via chiral transformation, the sum $\bar{\theta}$ is invariant.

The upper-bound of $\bar{\theta}$ is derived from the experimental upper bound on the electric dipole moment (edm) of the neutron as $|\bar{\theta}| \lesssim 10^{-10}$ [5]. This bound is much smaller than the weak CP violation, for example, the Jarlskog rephasing invariant $\sim 10^{-5}$ [6, 7]. Therefore, the strong CP problem is the problem of understanding why $\bar{\theta}$ is so small.

The most well known solution is the axion solution [8] (see also, e.g., [9]), where $\bar{\theta}$ is a dynamical degree of freedom which is set to a small value by a scalar potential. However, there have been no experimental hints for the existence of the axion so far.

Another well known solution is provided by the Nelson-Barr model [10, 11], where the CP symmetry is violated only by the mixings of Standard model (SM) quarks with hypothetical extra heavy quarks, and the extended quark mass matrix has a special structure with vanishing entries such that CP-violating terms do not contribute to its determinant. Specific models, in which quark mass matrices with real determinant and $\theta_{\text{QCD}} = 0$ still generate the weak CP-violating (CPV) phase in the CKM quark mixing matrix have been proposed in [12–24] as well.

The modular invariance opened up a new promising approach to the flavour problem of quarks and leptons [25] (see also Refs. [26–28]). The strong CP problem has been also discussed recently within the modular invariance approach in Ref. [29]. In this study a simple effective theory of flavour and CP symmetry breaking with vanishing $\bar{\theta}$ without the need for an axion has been proposed. The analysis was done using the level $N = 1$ full modular group $\text{SL}(2, \mathbb{Z})$. A numerical example has shown that the modular symmetry allows to solve the strong CP problem and to reproduce correctly the quark masses and the CKM mixing matrix.

In this article we present alternative effective quark flavour models with finite modular symmetry of level $N = 3$ (A_4), which provide axion-less solution to the strong CP problem. The A_4 modular symmetry has been extensively used for understanding the origins of the quark and lepton flavours [25, 30–44]. Finite groups including finite modular groups have been widely employed in flavour model building (see, e.g., [26–28, 45–53]¹ and the reviews [54–65]).

¹A rather complete list of articles on the modular invariance approach to lepton and quark flavour problems is given in [53].

If CP is a fundamental symmetry of the Lagrangian, the QCD and the strong CPV phases θ_{QCD} and $\bar{\theta}$ will vanish. However, in order to explain CP violation in weak interactions, the spontaneous breaking of the CP symmetry has to generate the large measured value of the CPV phase in the CKM matrix, while at the same time the strong CPV phase $\bar{\theta}$ should still be zero or be tiny enough to be in agreement with experimental data on the edm of the neutron. In other words, we have to look for a texture with $\arg \det [M_U M_D] = 0$ with a realistic value for the CKM CPV phase. Furthermore, as far as there is no accidental cancellation between phases in the up-type and down-type mass matrices, $\det [M_U]$ and $\det [M_D]$ should be real, and positive by themselves.

Since constraints of $\bar{\theta}$ are very stringent, we need to take into account the corrections to this parameter. The most important corrections are ² [19, 29]:

- Higher dimensional operators that spoil the structure of the mass matrices.
- Corrections which are induced from supersymmetry (SUSY) breaking terms.

The first point has been addressed by introducing the modular symmetry within the modular invariance approach to the quark (lepton) flavour problem [25], in which the elements of the quark (charged lepton and neutrino) mass matrices are modular forms of certain levels and weights that are holomorphic functions of the modulus τ . The modular forms are essentially non-perturbative ones. Once the weight of the modular form is fixed there are no the higher dimensional operator contributions. The symmetry is sharp.

The second point is the correction due to the SUSY breaking terms. This correction has been discussed in the modular symmetry of flavours [29]. Since the modular symmetry is in the framework of SUSY, the SUSY breaking could contribute to $\bar{\theta}$ significantly. As far as SUSY is unbroken, $\bar{\theta}$ cannot be generated radiatively. On the other hand, the SUSY breaking sector, in principle, can introduce new sources of CP violation which are model dependent. Assuming that SUSY is broken via gauge-mediation or anomaly-mediation below the mass scale of the modulus τ , the renormalization group and threshold corrections due to the SUSY breaking have same flavour and CP structure as the SM ones [13]. Therefore, the corrections to $\bar{\theta}$ are safely under control.

In the case of A_4 modular symmetry considered by us relevant texture zeros of the quark mass matrices are realized if both left-handed (LH) and right-handed (RH) quark fields are assigned to be A_4 singlets [68]. The CP violation is generated only by the vacuum expectation value (VEV) of the modulus τ [69]. By performing statistical analysis we obtain the values of the VEV of τ that allow to reproduce the observed CP violation in the quark sector.

It is known that the VEV of the modulus τ could be obtained by the modulus stabilisation analysing relatively simple (supergravity-motivated) modular- and CP-invariant potentials for the modulus τ . In the modulus stabilisation studies values of the VEV of τ close to the fixed points [45] i , ω and $i\infty$ were found [70–78]. In view of this we search in this work for examples of A_4 modular solutions to the strong CP problem for values of the VEV of τ close to the fixed points.

²The corrections to $\bar{\theta}$ from SM are known to be negligible [66, 67]

The paper is organised as follows. In Section 2, we present quark mass matrices with three types of texture zeros, which satisfy $\arg \det [M_Q] = 0$. In Section 3, we propose quark mass matrices with the considered texture zeros in the case of A_4 modular symmetry and discuss their CP violating phase structure. In Section 4, we show numerical examples which allow to reproduce the observed quark masses, CKM mixing angles and CP-violating phase for the VEV of τ close to the fixed points i , ω and $i\infty$. In Section 5, we focus on the VEV of τ , which gives the absolute minima of the supergravity-motivated modular- and CP-invariant potentials for the modulus τ , so called, modulus stabilisation. We present a successful model, which is consistent with the modulus stabilisation close to $\tau = \omega$ [73]. Section 6 is devoted to the summary and discussions. In Appendix A the A_4 modular forms of weights up to 16 are presented. In Appendix B we list the observed values of the quark masses, the CKM elements and CPV phase, which serve as input for our numerical analyses. In Appendix C we present numerically three examples of phenomenologically viable quark mass matrices with texture zeros that allow to describe the data on quark masses, mixing and CP violation.

2 Texture zeros and Real $\det [M_Q]$

The texture zeros approach has a long history. In Ref. [80] Weinberg, assuming the existence of two families of quarks, considered a mass matrix for the down-type quark sector with zero (1,1) entry in the basis in which the up-type quark mass matrix is diagonal. He further supposed that the down-type quark mass matrix is symmetric. In this case the number of free parameters is reduced to only two and hence he succeeded to predict the Cabibbo angle to be $\sqrt{m_d/m_s}$, which is the so-called Gatto, Sartori, Tonin relation [81]. Fritzsch extended the above approach to the three family case [82, 83]. Ramond, Roberts and Ross presented a systematic analysis with four or five zeros for symmetric or hermitian quark mass matrices [84]. Their textures are not viable today since they cannot describe the current rather precise data on the CKM quark mixing matrix. However, the texture zero approach to the quark mass matrices is still promising [85, 86]³.

A systematic study of texture zeros has been presented for the down-type quark mass matrix in the basis of diagonal up-type quark mass matrix in Ref. [90] from the standpoint of “Occam’s Razor approach” [91], in which a minimum number of parameters is allowed. The down-type quark mass matrix was arranged to have the minimum number of parameters by setting three of its elements to zero, while at the same time requiring that it describes successfully the CKM mixing and CP violation without assuming it to be symmetric or hermitian. Some of the texture zeros considered in Ref. [90] lead to real $\det [M_Q]$. For the purpose of our study, where the modular invariance of the quark mass matrices determines the texture zeros, we discuss three sets of texture zeros for both the down-type and up-type mass matrices, M_Q , which are texture

³By making a suitable weak basis transformation, one can obtain some sets of zeros of the quark mass matrices. This issue was discussed in Refs. [87–89]

zeros of the corresponding quark Yukawa couplings Y_Q ⁴: $M_Q = v_Q Y_Q$, $Q = D, U$, $v_{D,U}$ being the VEVs of the down-type and up-type doublet Higgs fields. In the right-left (RL) convention for the mass matrices $(M_Q)_{RL} = v_Q (Y_Q)_{RL}$, which we are going to employ in our analysis, the three sets of textures we were referring to above are:

$$\begin{aligned}
(1) : \quad Y_Q = v_Q^{-1} M_Q &= \begin{pmatrix} 0 & 0 & a_Q \\ 0 & b_Q & c_Q \\ d_Q & e_Q & f_Q e^{i\varphi_Q} \end{pmatrix}_{RL}, \\
(2) : \quad Y_Q = v_Q^{-1} M_Q &= \begin{pmatrix} 0 & 0 & a_Q \\ b_Q & 0 & c_Q \\ e_Q & d_Q & f_Q e^{i\varphi_Q} \end{pmatrix}_{RL}, \\
(3) : \quad Y_Q = v_Q^{-1} M_Q &= \begin{pmatrix} a_Q & 0 & 0 \\ c_Q & b_Q & 0 \\ f_Q e^{i\varphi_Q} & e_Q & d_Q \end{pmatrix}_{RL}, \tag{3}
\end{aligned}$$

where $Q = D, U$, and $a_Q, b_Q, c_Q, d_Q, e_Q, f_Q$ are real coefficients. The texture (1) is used in Ref. [29] for the discussion of the strong CP problem. The textures (2) and (3) are obtained by exchange of columns ($1 \leftrightarrow 2$) and ($1 \leftrightarrow 3$) of the matrix (1), respectively. The physics (the CKM matrix) is different among them. On the other hand, the physics is not changed by the exchange of the rows of (1) since it respects only the right-handed sector. The CPV phases φ_D and φ_U are assigned to specific entries so that the mass matrices in Eq. (3) coincide in form with those obtained from modular invariance in our further analysis. As we will see, the modular invariance constraints the down-type and up-type quark mass matrices we will consider to have each only one CPV phase originating from the VEV of the modulus τ . The determinants of the considered mass matrices are real:

$$\det [M_Q] = \pm a_Q b_Q d_Q. \tag{4}$$

We show typical examples of numerical fits for the three textures of Eq. (3) in Appendix C, for which the input data are given in Appendix B.

3 Realization of texture zeros in A_4 modular symmetry

We will present next modular invariant mass matrices with level $N = 3$ (A_4) modular symmetry. They have the texture zeros of the matrices given in Eq. (3). In order to realize the desirable texture zeros, all quarks should be assigned to A_4 singlets. However, the modular forms representing trivial singlets $\mathbf{1}$ are just equivalent to the Eisenstein series, which correspond to the modular forms of

⁴There are thirteen available textures with three zeros, of which six textures lead to real $\det [M_Q]$ [90]. They give three different relations between the CKM angles and the quark masses as seen in Table 1 of Ref. [90]. The three textures in Eq. (3) are representatives of the indicated six textures.

level $N = 1$ modular symmetry, as shown in Eq.(61) of Appendix A. An example of modular invariant mass matrix with level $N = 1$ modular symmetry was presented in Ref. [29]. In this work, we employ modular forms that are non-trivial singlets $\mathbf{1}'$ and $\mathbf{1}''$ in addition to forms which are trivial singlets $\mathbf{1}$. In order to reproduce the observed CP violation of the quark sector, two singlet modular forms with same weight furnishing the same singlet representation are required to avoid the vanishing of the CPV phase due to cancellation between the contributions for the down-type and up-type quark mass matrices. The smallest weight k_Y at which there exists two A_4 modular forms of the same singlet representation is $k_Y = 12$, but the forms are trivial $\mathbf{1}$ singlets. Two non-trivial $\mathbf{1}'$ singlet modular forms of the same weight exist at $k_Y = 16$ and at larger weights, as seen in Appendix A. In this section, using two $\mathbf{1}'$ singlet modular forms with weight $k = 16$ together with additional singlet modular forms, we construct quark mass matrices with A_4 modular symmetry, which have the general forms given in Eq.(3).

3.1 Quark mass matrix of model (1) and its CPV phase structure

In order to keep $\det [M_D M_U]$ to be real, the following condition of the weights are required [29]:

$$\sum_{i=1}^3 (2k_{Q_i} + k_{d_i}^c + k_{u_i}^c) = 0, \quad (5)$$

where k_{Q_i} and $k_{d_i}^c (k_{u_i}^c)$ denote weights for the left-handed quarks and right-handed down (up)-type quarks, respectively. The weights of Higgs are set to be zero. The condition of Eq.(5) guarantees that the modular symmetry has no QCD anomaly.

We assign the A_4 representations and the weights for quarks and Higgs as follows:

- quark doublet (left-handed) $Q_1 = (d, u)_L, Q_2 = (s, c)_L, Q_3 = (b, t)_L$: A_4 singlets $(1, 1, 1'')$ with weight $(-8, -4, 8)$.
- quark singlets (right-handed) (d^c, s^c, b^c) and (u^c, c^c, t^c) : A_4 singlets $(1', 1, 1)$ with weight $(-8, 4, 8)$, respectively.
- Higgs fields of down-type and up-type quark sectors $H_{U,D}$: A_4 singlet 1 with weight 0 .

The assigned weights satisfy the condition in Eq.(5). These assignments are summarized in Table 1.

Taking account of the following tensor products of A_4 singlets [55–57],

$$\mathbf{1} \otimes \mathbf{1} = \mathbf{1}, \quad \mathbf{1}' \otimes \mathbf{1}' = \mathbf{1}'', \quad \mathbf{1}'' \otimes \mathbf{1}'' = \mathbf{1}', \quad \mathbf{1}' \otimes \mathbf{1}'' = \mathbf{1}, \quad (6)$$

the superpotential terms w_D and w_U of the down-type and up-type quark superfields with weights

	$(d, u)_L, (s, c)_L, (b, t)_L$	$(d^c, s^c, b^c), (u^c, c^c, t^c)$	H_U	H_D
$SU(2)$	2	1	2	2
A_4	$(1, 1, 1'')$	$(1', 1, 1)$	1	1
k	$(-8, -4, 8)$	$(-8, 4, 8)$	0	0

Table 1: Assignments of A_4 representations and weights in model (1). We note that the exponent in the automorphy factor in the modular transformations of the quark superfields we work with is $(-k)$.

as given in Table 1 read:

$$\begin{aligned}
w_D &= \left[a_D d^c Q_3 + b_D s^c Q_2 + c_D s^c Q_3 Y_{\mathbf{1}'}^{(12)} + d_D b^c Q_1 + e_D b^c Q_2 Y_{\mathbf{1}}^{(4)} + f_D b^c Q_3 (g_D Y_{\mathbf{1}'A}^{(16)} + Y_{\mathbf{1}'B}^{(16)}) \right] H_D, \\
w_U &= \left[a_U u^c Q_3 + b_U c^c Q_2 + c_U c^c Q_3 Y_{\mathbf{1}'}^{(12)} + d_U t^c Q_1 + e_U t^c Q_2 Y_{\mathbf{1}}^{(4)} + f_U t^c Q_3 (g_U Y_{\mathbf{1}'A}^{(16)} + Y_{\mathbf{1}'B}^{(16)}) \right] H_U,
\end{aligned} \tag{7}$$

where $Y_{\mathbf{r}}^{(k_Y)}$ are modular forms of $\mathbf{r} = \mathbf{1}, \mathbf{1}'$ with weight k_Y as seen in Appendix A. Parameters $a_D, b_D, c_D, d_D, e_D, f_D, g_D$ and $a_U, b_U, c_U, d_U, e_U, f_U, g_U$ are constants. These constants are real as a consequence of the imposed CP invariance of the Lagrangian of the theory. We note that w_D and w_U involve three modular forms that are $\mathbf{1}'$ singlets, $Y_{\mathbf{1}'}^{(12)}, Y_{\mathbf{1}'A}^{(16)}$ and $Y_{\mathbf{1}'B}^{(16)}$, in addition to the trivial singlet one $Y_{\mathbf{1}}^{(4)}$.

The Yukawa matrices of the down-type and up-type quarks follow from the expressions for w_D and w_U and are given by:

$$Y_D = \begin{pmatrix} 0 & 0 & a_D \\ 0 & b_D & c_D Y_{\mathbf{1}'}^{(12)} \\ d_D & e_D Y_{\mathbf{1}}^{(4)} & f_D (g_D Y_{\mathbf{1}'A}^{(16)} + Y_{\mathbf{1}'B}^{(16)}) \end{pmatrix}_{RL}, \quad Y_U = \begin{pmatrix} 0 & 0 & a_U \\ 0 & b_U & c_U Y_{\mathbf{1}'}^{(12)} \\ d_U & e_U Y_{\mathbf{1}}^{(4)} & f_U (g_U Y_{\mathbf{1}'A}^{(16)} + Y_{\mathbf{1}'B}^{(16)}) \end{pmatrix}_{RL}. \tag{8}$$

We take the modular invariant kinetic terms simply as ⁵

$$\sum_I \frac{|\partial_\mu \psi^{(I)}|^2}{\langle -i\tau + i\bar{\tau} \rangle^{k_I}}, \tag{9}$$

where $\psi^{(I)}$ denotes a chiral superfield with weight k_I , and $\bar{\tau}$ is the anti-holomorphic modulus. The (anti-)holomorphic modulus is a dynamical field. It becomes a complex number after the modulus τ takes a VEV. Then, one can set $\bar{\tau} = \tau^*$.

⁵Possible non-minimal additions to the Kähler potential, compatible with the modular symmetry, may jeopardise the predictive power of the approach [92]. However, those do not affect $\arg \det M_Q$ as discussed in Ref. [29].

It is important to address the transformation needed to get the kinetic terms of matter superfields in canonical form because the terms in Eq. (9) are not canonical. The canonical form is obtained by an overall re-normalization of the quark superfields of interest:

$$\psi^{(I)} \rightarrow \sqrt{(2\text{Im}\tau_q)^{k_I}} \psi^{(I)}. \quad (10)$$

This changes some of the constant parameters in the quark mass matrices in the following way:

$$\begin{aligned} c_Q &\rightarrow \hat{c}_Q = c_Q \sqrt{(2\text{Im}\tau)^{12}} = c_Q (2\text{Im}\tau)^6, \\ e_Q &\rightarrow \hat{e}_Q = e_Q \sqrt{(2\text{Im}\tau)^4} = e_Q (2\text{Im}\tau)^2, \\ f_Q &\rightarrow \hat{f}_Q = f_Q \sqrt{(2\text{Im}\tau)^{16}} = f_Q (2\text{Im}\tau)^8, \quad Q = D, U. \end{aligned} \quad (11)$$

The constants a_Q , b_Q , d_Q remain unchanged. Thus, the mass matrices of the down-type and up-type quarks take the form:

$$\begin{aligned} M_D &= v_D \begin{pmatrix} 0 & 0 & a_D \\ 0 & b_D & c_D (2\text{Im}\tau)^6 Y_{\mathbf{1}'}^{(12)} \\ d_D & e_D (2\text{Im}\tau)^2 Y_{\mathbf{1}}^{(4)} & f_D (2\text{Im}\tau)^8 (g_D Y_{\mathbf{1}'A}^{(16)} + Y_{\mathbf{1}'B}^{(16)}) \end{pmatrix}_{RL}, \\ M_U &= v_U \begin{pmatrix} 0 & 0 & a_U \\ 0 & b_U & c_U (2\text{Im}\tau)^6 Y_{\mathbf{1}'}^{(12)} \\ d_U & e_U (2\text{Im}\tau)^2 Y_{\mathbf{1}}^{(4)} & f_U (2\text{Im}\tau)^8 (g_U Y_{\mathbf{1}'A}^{(16)} + Y_{\mathbf{1}'B}^{(16)}) \end{pmatrix}_{RL}. \end{aligned} \quad (12)$$

The determinants of the quark mass matrices M_D and M_U given in the preceding equation are real:

$$\det[M_D] = -a_D b_D d_D, \quad \det[M_U] = -a_U b_U d_U. \quad (13)$$

The phase structure of the matrices in Eq. (12) is rather simple. The CP violating phases originate from the VEV of the modulus τ via the modular forms $Y_{\mathbf{1}}^{(4)}$, $Y_{\mathbf{1}'}^{(12)}$, $Y_{\mathbf{1}'A}^{(16)}$ and $Y_{\mathbf{1}'B}^{(16)}$. The phases of $Y_{\mathbf{1}}^{(4)}$ and $Y_{\mathbf{1}'}^{(12)}$ in the (2, 3) and (3, 2) elements can be factorised as follows:

$$\begin{aligned} M_D &= v_D P_R^* \begin{pmatrix} 0 & 0 & a_D \\ 0 & b_D & c_D (2\text{Im}\tau)^6 |Y_{\mathbf{1}'}^{(12)}| \\ d_D & e_D (2\text{Im}\tau)^2 |Y_{\mathbf{1}}^{(4)}| & f_D (2\text{Im}\tau)^8 (g_D Y_{\mathbf{1}'A}^{(16)} + Y_{\mathbf{1}'B}^{(16)}) e^{-i(\varphi_4 + \varphi_{12})} \end{pmatrix} P_L, \\ M_U &= v_U P_R^* \begin{pmatrix} 0 & 0 & a_U \\ 0 & b_U & c_U (2\text{Im}\tau)^6 |Y_{\mathbf{1}'}^{(12)}| \\ d_U & e_U (2\text{Im}\tau)^2 |Y_{\mathbf{1}}^{(4)}| & f_U (2\text{Im}\tau)^8 (g_U Y_{\mathbf{1}'A}^{(16)} + Y_{\mathbf{1}'B}^{(16)}) e^{-i(\varphi_4 + \varphi_{12})} \end{pmatrix} P_L. \end{aligned} \quad (14)$$

The phase matrices P_R and P_L are given by:

$$P_R = \begin{pmatrix} e^{i\varphi_{12}} & 0 & 0 \\ 0 & 1 & 0 \\ 0 & 0 & e^{-i\varphi_4} \end{pmatrix}, \quad P_L = \begin{pmatrix} e^{-i\varphi_4} & 0 & 0 \\ 0 & 1 & 0 \\ 0 & 0 & e^{i\varphi_{12}} \end{pmatrix}, \quad (15)$$

where

$$\varphi_4 \equiv \arg Y_{\mathbf{1}}^{(4)}, \quad \varphi_{12} \equiv \arg Y_{\mathbf{1}'}^{(12)}. \quad (16)$$

The matrix P_R does not appear in the CKM mixing matrix. Since P_L is common in down-type quark and up-type quark mass matrices, the phase matrix P_L is cancelled out in the CKM matrix due to $P_L^* P_L = 1$. Thus, the CP violation originates from the phases of the (3, 3) elements of M_D and M_U in Eq. (14):

$$\arg [(g_D Y_{\mathbf{1}'A}^{(16)} + Y_{\mathbf{1}'B}^{(16)}) e^{-i(\varphi_4 + \varphi_{12})}] \equiv \Phi_D^{(1)}, \quad \arg [(g_U Y_{\mathbf{1}'A}^{(16)} + Y_{\mathbf{1}'B}^{(16)}) e^{-i(\varphi_4 + \varphi_{12})}] \equiv \Phi_U^{(1)}. \quad (17)$$

These phases are fixed by the values of the VEV of modulus τ and of the real parameters g_D and g_U . Due to the two $\mathbf{1}'$ singlet weight 16 modular forms, non-trivial CP-violating phases appear in down-type and up-type quark mass matrices as well as in the CKM matrix.

In Appendix C.1 we show that the mass matrices M_Q , $Q = D, U$, given in Eq. (14), which correspond to the first (upper) matrix of Yukawa couplings in Eq. (3), are completely consistent with the observed quark masses and CKM quark mixing and CP violation when their elements have the numerical values reported in Eq. (70) of Appendix C.1 and the CPV phases in the (3,3) elements in M_D and M_U have the values 24.36° and -150.26° , respectively. This implies that the quark matrices in Eq. (14), obtained using the A_4 modular invariance, could be consistent with the data on quark masses, mixing and CP violation if the phases $\Phi_D^{(1)}$ and $\Phi_U^{(1)}$ in Eq. (17) have the indicated values. If we will be able to adjust the VEV of the modulus τ and the values of the real constants g_D and g_U so that the phases $\Phi_D^{(1)}$ and $\Phi_U^{(1)}$ get these values, we will have viable quark mass matrices since the constants $a_D, b_D, c_D, d_D, e_D, f_D$ and $a_U, b_U, c_U, d_U, e_U, f_U$ can be used to reproduce the numerical values in the matrices in Eq. (70). These numerical values are derived by fitting the quark masses, the CKM matrix elements and the Jarlskog rephasing invariant J_{CP} quoted in Eqs. (62), (64) and (67) in Appendix B.

We plot in Fig. 1 the values of the modulus τ ⁶, which allow to reproduce the quoted numerical values of the CPV phases $\Phi_D^{(1)} = 24.36^\circ$ and $\Phi_U^{(1)} = -150.26^\circ$ within 1% deviation by scanning g_D and g_U in the ranges of $|g_D|, |g_U| = 0 - 0.5$ (blue points), $|g_D|, |g_U| = 0.5 - 2$ (red points) and $|g_D|, |g_U| = 2 - 10$ (magenta points). These ranges are chosen in order to illustrate the g_D and g_U dependences. As is indicated by the figure, there is a viable region of values of τ up to $\text{Im } \tau \simeq 2$. We find a region near the fixed points $\tau = \omega$ that is also viable. Indeed, in subsection 4.1 we easily obtain an example of a parameter set near the fixed points $\tau = \omega$ which provides a good description of the quark data. There is scarcely a viable point close to $\tau = i$.

In Fig. 2 we show the corresponding region in the $g_D - \text{Im } \tau$ plane for values of $|g_D|, |g_U| < 10$. The imaginary part of τ can have relatively large values $\text{Im } \tau \cong (1.5 - 2.0)$ in the region of $|g_D| < 0.5$, the maximal value $\text{Im } \tau \cong 2.0$ being reached for $|g_D| \ll 1$. We do not show the analogous plot in the $g_U - \text{Im } \tau$ plane since it is almost the same as the one in Fig. 2.

⁶By “values of the modulus τ ” here and in what follows we mean “values of the VEV of the modulus τ ”.

We will present in subsection 4.1 the results of the fits of the the quark masses, CKM elements and the Jarlskog rephasing invariant J_{CP} quoted in Eqs. (62), (64) and (67) of Appendix B.

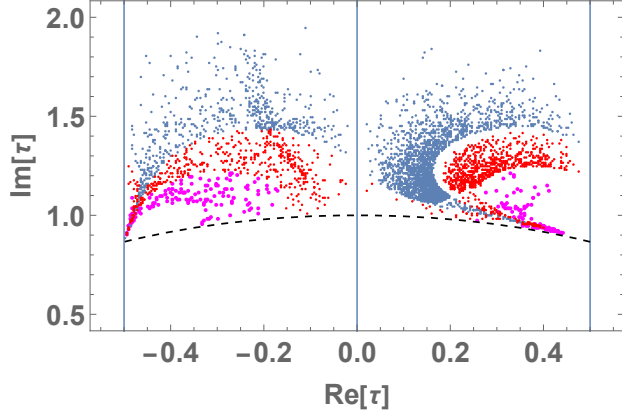


Figure 1: The region in $\text{Re}\tau$ - $\text{Im}\tau$ plane consistent with with observed CP phase of CKM matrix in model (1). Blue, red and magenta points correspond to $|g_D|, |g_U| = 0$ -0.5, 0.5-2 and 2-10, respectively.

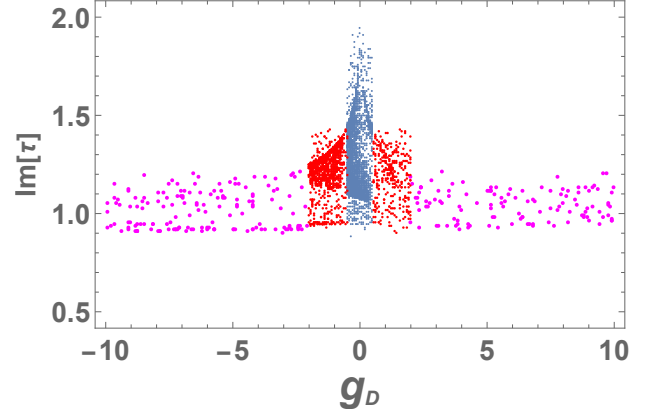


Figure 2: The region in g_D - $\text{Im}\tau$ plane consistent with observed CP phase of CKM matrix in model (1). Blue, red and magenta points correspond to $|g_D|, |g_U| = 0$ -0.5, 0.5-2 and 2-10, respectively.

Let us compare the allowed region obtained by us in the A_4 modular model with quark mass matrices given in Eq. (14) with that in the model proposed in Ref. [29], in which modular forms of level $N = 1$ modular symmetry are used. These modular forms are $\text{SL}(2, \mathbb{Z})$ singlets - the Eisenstein series with weight 4, 8 and 12, E_4 , E_8 and E_{12A} , E_{12B} . They coincide with the singlet $\mathbf{1}$ modular forms of the A_4 modular group of the same weights: $E_4 \equiv Y_1^{(4)}$, $E_8 \equiv Y_1^{(8)} = E_4^2$, $E_{12A} = E_4^3 \equiv Y_{1A}^{(12)}$, $E_{12B} = E_6^2 - E_4^3 \equiv Y_{1B}^{(12)}$, where $E_6 \equiv Y_1^{(6)}$ and $Y_1^{(4)}$, $Y_1^{(6)}$, $Y_1^{(8)}$, $Y_{1A}^{(12)}$ and $Y_{1B}^{(12)}$ are given in Appendix A. The parameters g_D and g_U appear in the quark mass matrices of the model in the same way they appear in the Yukawa matrices in Eq. (8):

$$M_Q = v_Q \begin{pmatrix} 0 & 0 & a_Q \\ 0 & b_Q & c_Q (2\text{Im}\tau)^4 Y_1^{(8)} \\ d_Q & e_Q (2\text{Im}\tau)^2 Y_1^{(4)} & f_Q (2\text{Im}\tau)^6 (g_Q Y_{1A}^{(12)} + Y_{1B}^{(12)}) \end{pmatrix}_{RL}, \quad Q = D, U. \quad (18)$$

The results of this analysis performed by us are shown in Fig. 3 and Fig. 4. The distributions of τ and g_D are almost the same as those shown in Figs. 1 and 2 because the textures of M_D and M_U are the same in the two models. We will see later that the distributions of τ and g_D depend significantly on the textures of the quark mass matrices.

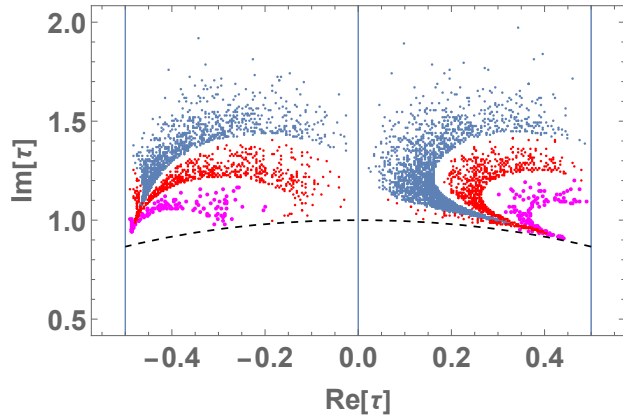


Figure 3: The region in $\text{Re } \tau$ - $\text{Im } \tau$ plane consistent with the observed CPV phase of CKM matrix in the case of $N = 1$ modular symmetry of the quark mass matrices, where Eisenstein series are used as modular forms [29]. Blue, red and magenta points correspond to $|g_D|, |g_U| = 0$ -0.5, 0.5-2 and 2-10, respectively. See the text for further details.

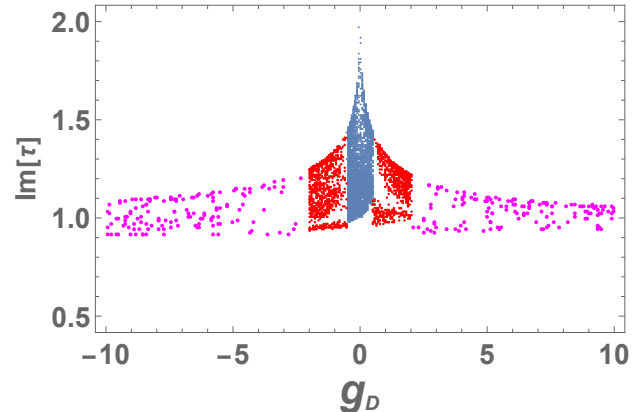


Figure 4: The region in g_D - $\text{Im } \tau$ plane consistent with observed CP phase of CKM matrix in the case of $N = 1$. Blue, red and magenta points correspond to $|g_D|, |g_U| = 0$ -0.5, 0.5-2 and 2-10, respectively.

3.2 Quark mass matrix of model (2) and its CPV phase structure

We present the second model (2), in which the assignments of the weights for the relevant chiral superfields are as follows:

- quark doublet (left-handed) $Q_1 = (d, u)_L, Q_2 = (s, c)_L, Q_3 = (b, t)_L$: A_4 singlets $(1, 1, 1'')$ with weight $(-4, -8, 8)$.
- quark singlets (right-handed) (d^c, s^c, b^c) and (u^c, c^c, t^c) : A_4 singlets $(1', 1, 1)$ with weight $(-8, 4, 8)$.
- Higgs fields of down-type and up-type quark sectors $H_{U,D}$: A_4 singlet 1 with weight 0.

These assignments satisfy the weight condition of Eq. (5). Those are summarized in Table 2.

	$(d, u)_L, (s, c)_L, (b, t)_L$	$(d^c, s^c, b^c), (u^c, c^c, t^c)$	H_U	H_D
$SU(2)$	2	1	2	2
A_4	$(1, 1, 1'')$	$(1', 1, 1)$	1	1
k	$(-4, -8, 8)$	$(-8, 4, 8)$	0	0

Table 2: Assignments of A_4 representations and weights in model (2).

The mass matrices of the down-type and up-type quarks read:

$$M_Q = v_Q \begin{pmatrix} 0 & 0 & a_Q \\ b_Q & 0 & c_Q(2\text{Im}\tau)^6 Y_{\mathbf{1}'}^{(12)} \\ e_Q(2\text{Im}\tau)^2 Y_{\mathbf{1}}^{(4)} & d_Q & f_Q(2\text{Im}\tau)^8 (g_Q Y_{\mathbf{1}'_A}^{(16)} + Y_{\mathbf{1}'_B}^{(16)}) \end{pmatrix}_{RL}, \quad Q = D, U. \quad (19)$$

The CP violating phases come from the modulus τ in modular forms of $Y_{\mathbf{1}}^{(4)}$, $Y_{\mathbf{1}'}^{(12)}$, $Y_{\mathbf{1}'_A}^{(16)}$ and $Y_{\mathbf{1}'_B}^{(16)}$. The phases of $Y_{\mathbf{1}}^{(4)}$ and $Y_{\mathbf{1}'}^{(12)}$ in the (2, 3) and (3, 1) elements can be factorised as follows:

$$M_Q = v_Q P_R^* \begin{pmatrix} 0 & 0 & a_Q \\ b_Q & 0 & c_Q(2\text{Im}\tau)^6 |Y_{\mathbf{1}'}^{(12)}| \\ e_Q(2\text{Im}\tau)^2 |Y_{\mathbf{1}}^{(4)}| & d_Q & f_Q(2\text{Im}\tau)^8 (g_Q Y_{\mathbf{1}'_A}^{(16)} + Y_{\mathbf{1}'_B}^{(16)}) e^{-i(\varphi_4 + \varphi_{12})} \end{pmatrix}_{RL} P_L, \quad Q = D, U. \quad (20)$$

The phase matrices P_R and P_L are given by:

$$P_R = \begin{pmatrix} e^{i\varphi_{12}} & 0 & 0 \\ 0 & 1 & 0 \\ 0 & 0 & e^{-i\varphi_4} \end{pmatrix}, \quad P_L = \begin{pmatrix} 1 & 0 & 0 \\ 0 & e^{-i\varphi_4} & 0 \\ 0 & 0 & e^{i\varphi_{12}} \end{pmatrix}, \quad (21)$$

where φ_4 and φ_{12} are defined in Eq.(16). As in the model (1), the matrix P_R does not contribute to the CKM mixing matrix, while P_L , being common to down-type quark and up-type quark mass matrices, is cancelled out in the CKM matrix. The CP violation is generated by the phases of the (3, 3) elements of M_D and M_U in Eq. (20),

$$\arg [(g_D Y_{\mathbf{1}'_A}^{(16)} + Y_{\mathbf{1}'_B}^{(16)}) e^{-i(\varphi_4 + \varphi_{12})}] \equiv \Phi_D^{(2)}, \quad \arg [(g_U Y_{\mathbf{1}'_A}^{(16)} + Y_{\mathbf{1}'_B}^{(16)}) e^{-i(\varphi_4 + \varphi_{12})}] \equiv \Phi_U^{(2)}, \quad (22)$$

which are determined by the VEV of the modulus τ and the real parameters g_D and g_U .

The analysis which follows is analogous to that performed for the model (1) in the preceding section. The second (middle) matrix of Yukawa couplings in Eq. (3) generates the quark mass matrices reported in Eq. (71) of Appendix C.2, which have the same structure as the the mass matrices in Eq. (20), obtained by employing the A_4 modular symmetry. It is shown in C.2 that these mass matrices successfully describe the data on the quark masses, mixing and CP violation if their elements have the numerical values given in Eq. (73) and the CPV phases in the (3,3) elements in M_D and M_U possess the values 104.84° and 56.63° , respectively. Reproducing the real numerical values of the elements of M_D and M_U reported in Eq. (73) using the constants $a_D, b_D, c_D, d_D, e_D, f_D$ and $a_U, b_U, c_U, d_U, e_U, f_U$, does not pose a problems. Thus, if we find values of the VEV of τ and of the real constants g_D and g_U that generate CPV phases $\Phi_D^{(2)} = 104.84^\circ$ and $\Phi_U^{(2)} = 56.63^\circ$, then the A_4 modular matrices M_D and M_U in Eq. (20) will be phenomenologically viable for the so found values of the modulus VEV and g_D and g_U .

We have performed the relevant analysis and show in Fig. 5 the region of values of the VEV of τ for which the phases $\Phi_D^{(2)} = 104.84^\circ$ and $\Phi_U^{(2)} = 56.63^\circ$ are reproduced within 1% deviation

by scanning g_D and g_U in the ranges of $|g_D|, |g_U| = 0 - 0.5$ (blue points), $|g_D|, |g_U| = 0.5 - 2$ (red points) and $|g_D|, |g_U| = 2 - 10$ (magenta points). The allowed points of τ are considerably reduced as compared with those in Fig. 1. However, there is still a viable region of values of τ close to $\text{Im } \tau = 1.9$. We also find a region near the fixed points $\tau = \omega$ that is also viable. Indeed, in subsection 4.2 we present an example of a parameter set near the fixed points $\tau = \omega$ as well as the ones close to $\tau = i$ and at the large $\text{Im } \tau$.

In Fig. 6 we show the corresponding region in the $g_D - \text{Im } \tau$ plane for values of $|g_D|, |g_U| < 10$. The imaginary part of τ reaches the value of 1.9 for $|g_D| \ll 1$. The analogous plot of $g_U - \text{Im } \tau$ plane is almost the same one as the one in Fig. 6 and we do not show it here.

We will present in subsection 4.2 the results of the fits of the the quark masses, CKM elements and the Jarlskog rephasing invariant J_{CP} quoted in Eqs. (62), (64) and (67) of Appendix B.

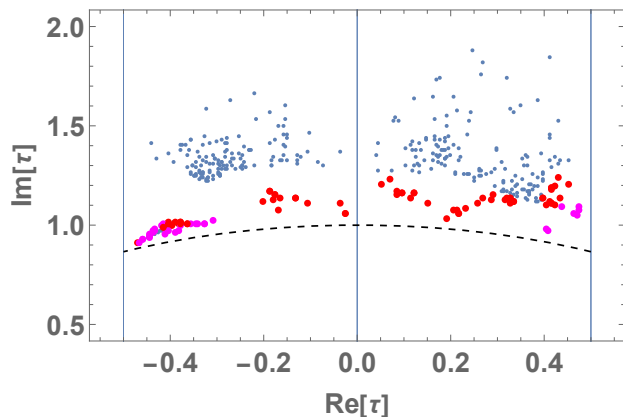


Figure 5: The region in $\text{Re } \tau - \text{Im } \tau$ plane consistent with with observed CP phase of CKM matrix in model (2). Blue, red and magenta points correspond to $|g_D|, |g_U| = 0-0.5$, $0.5-2$ and $2-10$, respectively.

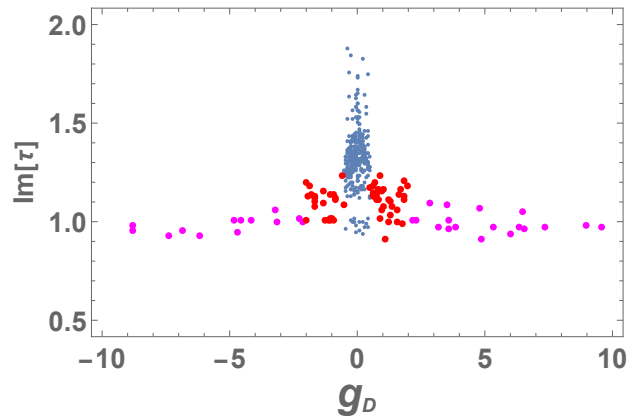


Figure 6: The region in $g_D - \text{Im } \tau$ plane consistent with observed CP phase of CKM matrix in model (2). Blue, red and magenta points correspond to $|g_D|, |g_U| = 0-0.5$, $0.5-2$ and $2-10$, respectively.

3.3 Quark mass matrix of model (3) and its CPV phase structure

For the model (3), the assignments of the weights for the relevant chiral superfields is given as follows:

- quark doublet (left-handed) $Q_1 = (d, u)_L, Q_2 = (s, c)_L, Q_3 = (b, t)_L$: A_4 singlets $(1'', 1, 1)$ with weight $(8, -4, -8)$.
- quark singlets (right-handed) (d^c, s^c, b^c) and (u^c, c^c, t^c) : A_4 singlets $(1', 1, 1)$ with weight $(-8, 4, 8)$.
- Higgs fields of down-type and up-type quark sectors $H_{U,D}$: A_4 singlet 1 with weight 0.

These assignments satisfy the weight condition of Eq.(5). Those are summarized in Table 3.

	$(d, u)_L, (s, c)_L, (b, t)_L$	$(d^c, s^c, b^c), (u^c, c^c, t^c)$	H_U	H_D
$SU(2)$	2	1	2	2
A_4	$(1'', 1, 1)$	$(1', 1, 1)$	1	1
k	$(8, -4, -8)$	$(-8, 4, 8)$	0	0

Table 3: Assignments of A_4 representations and weights in model (3).

The mass matrices of the down-type and up-type quarks have the form:

$$M_Q = v_Q \begin{pmatrix} a_Q & 0 & 0 \\ c_Q(2\text{Im}\tau)^6 Y_{1'}^{(12)} & b_Q & 0 \\ f_Q(2\text{Im}\tau)^8 (g_Q Y_{1'A}^{(16)} + Y_{1'B}^{(16)}) & e_Q(2\text{Im}\tau)^2 Y_1^{(4)} & d_Q \end{pmatrix}_{RL}, \quad Q = D, U. \quad (23)$$

Since the number of parameters are 14, four parameters are redundant for reproducing the quark masses and CKM elements (10 observables). In this case, following Ref. [90], we set $c_U = e_U = f_U = 0$ and we investigate whether one can describe successfully the quark data with this additional phenomenological assumption. As a consequence of setting the constants c_U , e_U and f_U to zero the up-type quark mass matrix is diagonal.

The CP violating phases originate from the modulus τ and appear in the down-type quark mass matrix M_D via the modular forms $Y_1^{(4)}$, $Y_{1'}^{(12)}$, $Y_{1'A}^{(16)}$ and $Y_{1'B}^{(16)}$. The phases of $Y_1^{(4)}$ and $Y_{1'}^{(12)}$ in the (2, 3) and (3, 1) elements can be factored out as follows:

$$M_D = v_D P_R^* \begin{pmatrix} a_D & 0 & 0 \\ c_D(2\text{Im}\tau)^6 |Y_{1'}^{(12)}| & b_D & 0 \\ f_D(2\text{Im}\tau)^8 (g_D Y_{1'A}^{(16)} + Y_{1'B}^{(16)}) e^{-i(\varphi_4 + \varphi_{12})} & e_D(2\text{Im}\tau)^2 |Y_1^{(4)}| & d_D \end{pmatrix}_{RL} P_L. \quad (24)$$

The phase matrices P_R and P_L are

$$P_R = P_L = \begin{pmatrix} 1 & 0 & 0 \\ 0 & e^{-i\varphi_{12}} & 0 \\ 0 & 0 & e^{-i(\varphi_4 + \varphi_{12})} \end{pmatrix}, \quad (25)$$

where φ_4 and φ_{12} are given in Eq. (16).

On the other hand, the up-type quark mass matrix is diagonal. Therefore, P_L and P_R do not contribute to the CKM matrix. Thus, the CP violation is generated by the phase of the (3, 1) element of M_D in Eq. (23),

$$\arg [(g_D Y_{1'A}^{(16)} + Y_{1'B}^{(16)}) e^{-i(\varphi_4 + \varphi_{12})}] \equiv \Phi_D^{(3)}, \quad (26)$$

which is determined by the VEV of τ and the real parameter g_D .

As shown in Eq. (74) of Appendix C.3, the quark mass matrices in Eq. (23) could be completely consistent with observed masses and the CKM matrix if the phase of Eq. (26) has the value $\Phi_D^{(3)} = 66.36^\circ$. By adjusting the value of the VEV of the modulus τ and of the real constant g_D to get $\Phi_D^{(3)} = 66.36^\circ$, we will obtain a phenomenologically viable down-quark mass matrix M_D . The real constants $a_D, b_D, c_D, d_D, e_D, f_D$ can be used to reproduce the real numerical values in M_D in Eq. (76).

We plot in Fig. 7 the values of the VEV of τ for which one can generate $\Phi_D^{(3)} = 66.36^\circ$ within 1% deviation by scanning g_D and g_U again in the ranges of $|g_D|, |g_U| = 0 - 0.5$ (blue points), $|g_D|, |g_U| = 0.5 - 2$ (red points) and $|g_D|, |g_U| = 2 - 10$ (magenta points). In the considered case it is possible to reproduce the observed CP violation in the quark sector even for τ close to ω and τ “close” to $i\infty$. Indeed, we present examples of viable parameter sets for $\tau \simeq \omega$ and $\text{Im } \tau \simeq 1.7$ in subsection 4.3.

In Fig. 8, we show the values of $\text{Im } \tau$ leading (within 1% deviation) to the requisite value of $\Phi_D^{(3)}$ versus $|g_D| < 10$. The magnitude of $\text{Im } \tau$ increases rapidly when $|g_D|$ decreases towards 0.

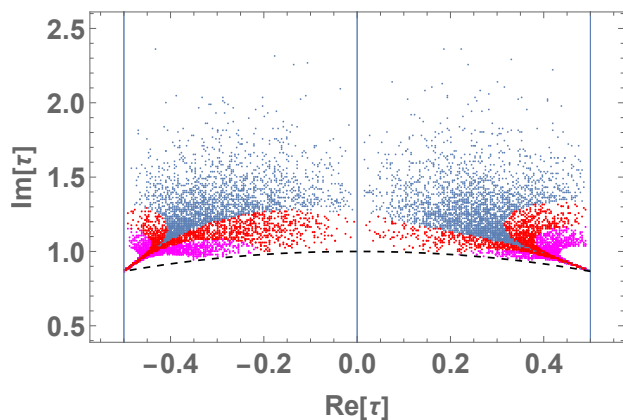


Figure 7: The region in $\text{Re } \tau$ - $\text{Im } \tau$ plane consistent with with observed CP phase of CKM matrix in model (3). Blue, red and magenta points correspond to $|g_D|, |g_U| = 0-0.5, 0.5-2$ and $2-10$, respectively.

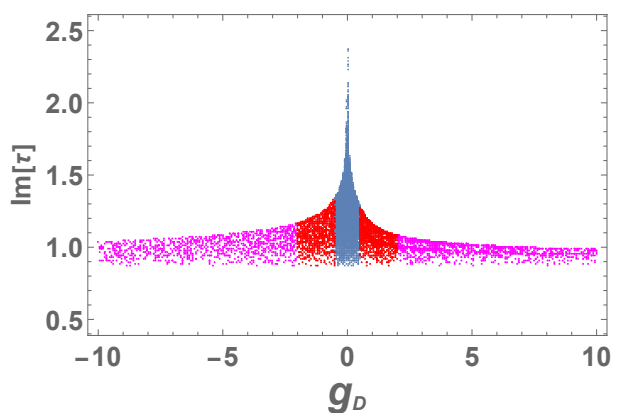


Figure 8: The region in g_D - $\text{Im } \tau$ plane consistent with observed CP phase of CKM matrix in model (3). Blue, red and magenta points correspond to $|g_D|, |g_U| = 0-0.5, 0.5-2$ and $2-10$, respectively.

Let us emphasise that in the case of the discussed model (3) we have set the redundant parameters $c_U = e_U = f_U = 0$ “by hand” to get diagonal mass matrix for the up-type quarks. This set-up is not guaranteed within the framework of the modular invariance approach without additional (symmetry) assumptions.

4 Reproducing quark masses and CKM parameters

We present next numerical examples of successfully reproducing the observed quark masses, the CKM mixing angles and CPV phase in the cases of the three models considered by us.

4.1 Fitting model (1)

We present three examples of model (1) corresponding to the τ being relatively close to the fixed points $\tau = i$, ω and ∞ , respectively.

4.1.1 τ close to i

The first one is an example of model (1), where τ is rather close to i . This case is comparable to the example in Ref. [29]. We show the numerical values of parameters obtained in the fit of the quark masses, CKM mixing angles, the CPV phase δ_{CP} and of the Jarlskog rephasing invariant J_{CP} [6], as defined in [7] and quoted in Eqs. (62), (64) and (67) of Appendix B:

$$\begin{aligned} \frac{b_D}{a_D} &= -0.724, & \frac{c_D}{a_D} &= 0.0430, & \frac{d_D}{a_D} &= 0.0864, & \frac{e_D}{a_D} &= 0.135, & \frac{f_D}{a_D} &= 0.00750, \\ \frac{b_U}{a_U} &= 0.972, & \frac{c_U}{a_U} &= 0.361, & \frac{d_U}{a_U} &= 0.631, & \frac{e_U}{a_U} &= 1.49, & \frac{f_U}{a_U} &= 0.154, \\ g_D &= -0.749, & g_U &= -1.10, & \tau &= 0.1811 + i 1.1583, & N\sigma &= 0.52, \end{aligned} \quad (27)$$

where $N\sigma$ denotes a measure of goodness of the fit. By employing the sum of one-dimensional $\Delta\chi^2$ for eight observable quantities m_d/m_b , m_s/m_b , m_u/m_t , m_c/m_t , $|V_{us}|$, $|V_{cb}|$, $|V_{ub}|$, δ_{CP} , it is defined as $N\sigma \equiv \sqrt{\Delta\chi^2}$. The result of the fit of the quark mass ratios, three CKM elements $|V_{us}|$, $|V_{cb}|$, $|V_{ub}|$, the phase δ_{CP} and of the J_{CP} factor are collected in Table 4.

	$\frac{m_s}{m_b} \times 10^2$	$\frac{m_d}{m_b} \times 10^4$	$\frac{m_c}{m_t} \times 10^3$	$\frac{m_u}{m_t} \times 10^6$	$ V_{us} $	$ V_{cb} $	$ V_{ub} $	$ J_{CP} $	δ_{CP}
Fit	1.87	8.84	2.80	5.89	0.2251	0.0401	0.00352	2.84×10^{-5}	66.8°
Exp	1.82	9.21	2.80	5.39	0.2250	0.0400	0.00353	2.80×10^{-5}	66.2°
1σ	± 0.10	± 1.02	± 0.12	± 1.68	± 0.0007	± 0.0008	± 0.00013	$^{+0.14}_{-0.12} \times 10^{-5}$	$^{+3.4^\circ}_{-3.6^\circ}$

Table 4: Results of the fits of the quark mass ratios, CKM mixing angles, J_{CP} and δ_{CP} . 'Exp' denotes the values of the observables at the GUT scale, including 1σ error.

We comment on the values of parameters in Eq. (27). The parameters a_Q , b_Q , d_Q ($Q = D, U$) are real constants that do not couple to modular forms. On the other hand, c_Q , e_Q , f_Q ($Q = D, U$) are constants multiplying the modular forms. Since the normalizations of each of the three modular forms present in the expressions for the quark mass matrices M_D and M_U are arbitrary, the

magnitudes of the parameters a_Q, b_Q, d_Q and respectively those of c_Q, e_Q, f_Q should be compared separately among themselves. The constants multiplying the modular forms are of the same order in magnitude:

$$\left| \frac{c_D}{f_D} \right| \simeq 5.7, \quad \left| \frac{e_D}{f_D} \right| \simeq 18, \quad \left| \frac{c_U}{f_U} \right| \simeq 2.3, \quad \left| \frac{e_U}{f_U} \right| \simeq 9.7. \quad (28)$$

In what concerns the constants, a_Q, b_Q, d_Q , only the ration $|d_D/a_D|$ is somewhat smaller than the other ratios $|b_D/a_D|, |b_U/a_U|$ and $|d_U/a_U|$:

$$\left| \frac{b_D}{a_D} \right| \simeq 0.72, \quad \left| \frac{d_D}{a_D} \right| \simeq 0.086, \quad \left| \frac{b_U}{a_U} \right| \simeq 0.97, \quad \left| \frac{d_U}{a_U} \right| \simeq 0.63. \quad (29)$$

4.1.2 τ close to ω

We present the second example of successful fit of the quark data, in which the VEV of the modulus τ is close to the fixed point $\omega = -0.5 + i\sqrt{3}/2$ (the left cusp). The numerical values of parameters read:

$$\begin{aligned} \frac{b_D}{a_D} &= 0.895, & \frac{c_D}{a_D} &= 0.816, & \frac{d_D}{a_D} &= 0.0830, & \frac{e_D}{a_D} &= 0.524, & \frac{f_D}{a_D} &= 0.00973, \\ \frac{b_U}{a_U} &= 1.26, & \frac{c_U}{a_U} &= 5.90, & \frac{d_U}{a_U} &= 0.667, & \frac{e_U}{a_U} &= 7.53, & \frac{f_U}{a_U} &= 0.264, \\ g_D &= -0.809, & g_U &= 3.33, & \tau &= -0.4900 + i0.9493, & \tau - \omega &= 0.0093 + i0.0832, & N\sigma &= 0.87. \end{aligned} \quad (30)$$

In Table 5 we present the results of the fit of the quark mass ratios, the three CKM elements $|V_{us}|, |V_{cb}|, |V_{ub}|$, of the CPV phase δ_{CP} and of the J_{CP} factor.

	$\frac{m_s}{m_b} \times 10^2$	$\frac{m_d}{m_b} \times 10^4$	$\frac{m_c}{m_t} \times 10^3$	$\frac{m_u}{m_t} \times 10^6$	$ V_{us} $	$ V_{cb} $	$ V_{ub} $	$ J_{CP} $	δ_{CP}
Fit	1.88	8.73	2.85	5.57	0.2252	0.0398	0.00349	2.80×10^{-5}	66.9°
Exp	1.82	9.21	2.80	5.39	0.2250	0.0400	0.00353	2.80×10^{-5}	66.2°
1σ	± 0.10	± 1.02	± 0.12	± 1.68	± 0.0007	± 0.0008	± 0.00013	$^{+0.14}_{-0.12} \times 10^{-5}$	$^{+3.4}_{-3.6}^\circ$

Table 5: Results of the fits of the quark mass ratios, CKM mixing angles, J_{CP} and δ_{CP} . 'Exp' denotes the values of the observables at the GUT scale, including 1σ error.

The ratios of the constants multiplying the modular forms are of the same order of magnitude:

$$\left| \frac{c_D}{f_D} \right| \simeq 83.8, \quad \left| \frac{e_D}{f_D} \right| \simeq 53.9, \quad \left| \frac{c_U}{f_U} \right| \simeq 22.3, \quad \left| \frac{e_U}{f_U} \right| \simeq 28.5. \quad (31)$$

In what concerns the other constants, only the ratio of $|d_D/a_D|$ is again somewhat smaller than the other ratios:

$$\left| \frac{b_D}{a_D} \right| \simeq 0.90, \quad \left| \frac{d_D}{a_D} \right| \simeq 0.083, \quad \left| \frac{b_U}{a_U} \right| \simeq 1.26, \quad \left| \frac{d_U}{a_U} \right| \simeq 0.67. \quad (32)$$

4.1.3 τ “close” to $i\infty$

We present the third example of successful fit of quark data, in which the VEV of the modulus τ has a relatively large imaginary part “close” to the fixed point $i\infty$. The numerical values of parameters read:

$$\begin{aligned} \frac{b_D}{a_D} &= -0.469, & \frac{c_D}{a_D} &= 0.0138, & \frac{d_D}{a_D} &= 0.0581, & \frac{e_D}{a_D} &= 0.0296, & \frac{f_D}{a_D} &= 0.0497, \\ \frac{b_U}{a_U} &= 1.585, & \frac{c_U}{a_U} &= 0.0867, & \frac{d_U}{a_U} &= 2.504, & \frac{e_U}{a_U} &= 0.601, & \frac{f_U}{a_U} &= 4.282, \\ g_D &= 0.000130, & g_U &= -0.00316, & \tau &= 0.1097 + i 1.8213, & N\sigma &= 1.31. \end{aligned} \quad (33)$$

In Table 6 we present the results of the fit of the quark mass ratios, the three CKM elements $|V_{us}|$, $|V_{cb}|$, $|V_{ub}|$, of the CPV phase δ_{CP} and of the J_{CP} factor.

	$\frac{m_s}{m_b} \times 10^2$	$\frac{m_d}{m_b} \times 10^4$	$\frac{m_c}{m_t} \times 10^3$	$\frac{m_u}{m_t} \times 10^6$	$ V_{us} $	$ V_{cb} $	$ V_{ub} $	$ J_{CP} $	δ_{CP}
Fit	1.88	9.71	2.82	3.44	0.2248	0.0401	0.00353	2.84×10^{-5}	66.6°
Exp	1.88	8.72	2.80	5.39	0.2250	0.0400	0.00353	2.80×10^{-5}	66.2°
1σ	± 0.10	± 1.02	± 0.12	± 1.68	± 0.0007	± 0.0008	± 0.00013	$^{+0.14}_{-0.12} \times 10^{-5}$	$^{+3.4^\circ}_{-3.6^\circ}$

Table 6: Results of the fits of the quark mass ratios, CKM mixing angles, J_{CP} and δ_{CP} . ‘Exp’ denotes the values of the observables at the GUT scale, including 1σ error.

The constants multiplying the modular forms present in M_D and in M_U are of the same order of magnitude except for $|c_U/f_U|$, which is somewhat smaller than $|e_U/f_U|$:

$$\left| \frac{c_D}{f_D} \right| \simeq 0.28, \quad \left| \frac{e_D}{f_D} \right| \simeq 0.59, \quad \left| \frac{c_U}{f_U} \right| \simeq 0.02, \quad \left| \frac{e_U}{f_U} \right| \simeq 0.14. \quad (34)$$

In what concerns the other constants in M_D and in M_U , the ratio of $|d_D/a_D|$ is somewhat smaller than $|b_D/a_D|$, the other ratios $|b_U/a_U|$ and $|d_U/a_U|$ being of the same order of magnitude:

$$\left| \frac{b_D}{a_D} \right| \simeq 0.47, \quad \left| \frac{d_D}{a_D} \right| \simeq 0.058, \quad \left| \frac{b_U}{a_U} \right| \simeq 1.59, \quad \left| \frac{d_U}{a_U} \right| \simeq 2.50. \quad (35)$$

4.2 Fitting model (2)

We present three examples of model (2) corresponding to the τ being relatively close to the fixed points $\tau = i$, ω and ∞ , respectively.

4.2.1 τ close to i

The first example is close to $\tau = i$. For the numerical values of parameters resulting from the fit, we obtain in this case:

$$\begin{aligned} \frac{b_D}{a_D} &= -0.0541, & \frac{c_D}{a_D} &= 0.0212, & \frac{d_D}{a_D} &= 0.871, & \frac{e_D}{a_D} &= 0.0114, & \frac{f_D}{a_D} &= 0.0157, \\ \frac{b_U}{a_U} &= 5.58 \times 10^{-3}, & \frac{c_U}{a_U} &= 5.76 \times 10^{-2}, & \frac{d_U}{a_U} &= 1.63, & \frac{e_U}{a_U} &= 5.10 \times 10^{-4}, & \frac{f_U}{a_U} &= 1.11 \times 10^{-1}, \\ g_D &= 1.363, & g_U &= 1.151, & \tau &= 0.1706 + i 1.1417, & N\sigma &= 0.82. \end{aligned} \quad (36)$$

The results of the fit of the observables are shown in Table 7.

	$\frac{m_s}{m_b} \times 10^2$	$\frac{m_d}{m_b} \times 10^4$	$\frac{m_c}{m_t} \times 10^3$	$\frac{m_u}{m_t} \times 10^6$	$ V_{us} $	$ V_{cb} $	$ V_{ub} $	$ J_{CP} $	δ_{CP}
Fit	1.87	9.10	2.80	6.47	0.2250	0.0400	0.00360	2.86×10^{-5}	65.6°
Exp	1.82	9.21	2.80	5.39	0.2250	0.0400	0.00353	2.80×10^{-5}	66.2°
1σ	± 0.10	± 1.02	± 0.12	± 1.68	± 0.0007	± 0.0008	± 0.00013	${}^{+0.14}_{-0.12} \times 10^{-5}$	${}^{+3.4}_{-3.6}^\circ$

Table 7: Results of the fits of the quark mass ratios, CKM mixing angles, J_{CP} and δ_{CP} . 'Exp' denotes the values of the observables at the GUT scale, including 1σ error.

The constants multiplying the modular forms are of the same order of magnitude except for e_U , which is significantly smaller:

$$\left| \frac{c_D}{f_D} \right| \simeq 1.35, \quad \left| \frac{e_D}{f_D} \right| \simeq 0.73, \quad \left| \frac{c_U}{f_U} \right| \simeq 0.52, \quad \left| \frac{e_U}{f_U} \right| \simeq 0.0046. \quad (37)$$

The other constants are hierarchical:

$$\left| \frac{b_D}{a_D} \right| \simeq 0.054, \quad \left| \frac{d_D}{a_D} \right| \simeq 0.87, \quad \left| \frac{b_U}{a_U} \right| \simeq 0.0056, \quad \left| \frac{d_U}{a_U} \right| \simeq 1.63. \quad (38)$$

4.2.2 τ close to ω

We present the second example, in which the VEV of the modulus τ is close to the fixed point ω . The numerical values of parameters obtained in the fit are:

$$\begin{aligned} \frac{b_D}{a_D} &= 0.0505, & \frac{c_D}{a_D} &= -0.278, & \frac{d_D}{a_D} &= 0.839, & \frac{e_D}{a_D} &= 0.0317, & \frac{f_D}{a_D} &= -0.00963, \\ \frac{b_U}{a_U} &= 4.75 \times 10^{-3}, & \frac{c_U}{a_U} &= 0.889, & \frac{d_U}{a_U} &= 1.72, & \frac{e_U}{a_U} &= -1.89 \times 10^{-3}, & \frac{f_U}{a_U} &= -6.34 \times 10^{-2}, \\ g_D &= 1.64, & g_U &= -0.840, & \tau &= -0.4474 + i 0.9357, & \tau - \omega &= 0.0526 + i 0.0697, & N\sigma &= 0.96. \end{aligned} \quad (39)$$

The results of the fit of the observables are shown in Table 8.

	$\frac{m_s}{m_b} \times 10^2$	$\frac{m_d}{m_b} \times 10^4$	$\frac{m_c}{m_t} \times 10^3$	$\frac{m_u}{m_t} \times 10^6$	$ V_{us} $	$ V_{cb} $	$ V_{ub} $	$ J_{CP} $	δ_{CP}
Fit	1.89	9.27	2.86	4.48	0.2252	0.0400	0.00349	2.76×10^{-5}	64.7°
Exp	1.82	9.21	2.80	5.39	0.2250	0.0400	0.00353	2.80×10^{-5}	66.2°
1σ	± 0.10	± 1.02	± 0.12	± 1.68	± 0.0007	± 0.0008	± 0.00013	$^{+0.14}_{-0.12} \times 10^{-5}$	$^{+3.4^\circ}_{-3.6^\circ}$

Table 8: Results of the fits of the quark mass ratios, CKM mixing angles, J_{CP} and δ_{CP} . ‘Exp’ denotes the values of the observables at the GUT scale, including 1σ error.

The constants multiplying the modular forms are of the same order of magnitude except for e_U , which is significantly smaller also in this case:

$$\left| \frac{c_D}{f_D} \right| \simeq 28, \quad \left| \frac{e_D}{f_D} \right| \simeq 3.3, \quad \left| \frac{c_U}{f_U} \right| \simeq 14, \quad \left| \frac{e_U}{f_U} \right| \simeq 0.030. \quad (40)$$

The other constants are hierarchical:

$$\left| \frac{b_D}{a_D} \right| \simeq 0.051, \quad \left| \frac{d_D}{a_D} \right| \simeq 0.84, \quad \left| \frac{b_U}{a_U} \right| \simeq 0.0048, \quad \left| \frac{d_U}{a_U} \right| \simeq 1.72. \quad (41)$$

4.2.3 τ “close” to $i\infty$

We present the third example at the VEV of τ having a relatively large imaginary part “close” to $i\infty$. The numerical values of parameters obtained in the fit are:

$$\begin{aligned} \frac{b_D}{a_D} &= 1.07 \times 10^{-2}, & \frac{c_D}{a_D} &= -4.96 \times 10^{-3}, & \frac{d_D}{a_D} &= -0.166, & \frac{e_D}{a_D} &= 2.35 \times 10^{-3}, & \frac{f_D}{a_D} &= 5.38 \times 10^{-3}, \\ \frac{b_U}{a_U} &= 1.58 \times 10^{-4}, & \frac{c_U}{a_U} &= 2.99 \times 10^{-3}, & \frac{d_U}{a_U} &= 0.465, & \frac{e_U}{a_U} &= -6.98 \times 10^{-6}, & \frac{f_U}{a_U} &= -4.11 \times 10^{-2}, \\ g_D &= 0.124, & g_U &= -0.0709, & \tau &= 0.3102 + i 1.5672, & N\sigma &= 0.774. \end{aligned} \quad (42)$$

The results of the fit of the observables are shown in Table 9.

	$\frac{m_s}{m_b} \times 10^2$	$\frac{m_d}{m_b} \times 10^4$	$\frac{m_c}{m_t} \times 10^3$	$\frac{m_u}{m_t} \times 10^6$	$ V_{us} $	$ V_{cb} $	$ V_{ub} $	$ J_{CP} $	δ_{CP}
Fit	1.87	9.79	2.79	5.96	0.2250	0.0402	0.00352	2.82×10^{-5}	65.3°
Exp	1.82	9.21	2.80	5.39	0.2250	0.0400	0.00353	2.80×10^{-5}	66.2°
1σ	± 0.10	± 1.02	± 0.12	± 1.68	± 0.0007	± 0.0008	± 0.00013	$^{+0.14}_{-0.12} \times 10^{-5}$	$^{+3.4}_{-3.6}^\circ$

Table 9: Results of the fits of the quark mass ratios, CKM mixing angles, J_{CP} and δ_{CP} . 'Exp' denotes the values of the observables at the GUT scale, including 1σ error.

The constants multiplying the modular forms are of the same order of magnitude for the down-type quarks, but hierarchical for up-type quarks:

$$\left| \frac{c_D}{f_D} \right| \simeq 0.92, \quad \left| \frac{e_D}{f_D} \right| \simeq 0.44, \quad \left| \frac{c_U}{f_U} \right| \simeq 0.073, \quad \left| \frac{e_U}{f_U} \right| \simeq 0.00017. \quad (43)$$

The other constants are hierarchical:

$$\left| \frac{b_D}{a_D} \right| \simeq 0.011, \quad \left| \frac{d_D}{a_D} \right| \simeq 0.17, \quad \left| \frac{b_U}{a_U} \right| \simeq 0.00016, \quad \left| \frac{d_U}{a_U} \right| \simeq 0.47. \quad (44)$$

4.3 Fitting model (3)

We present three examples of model (3) corresponding to the τ being relatively close to the fixed points $\tau = i$, ω and ∞ , respectively.

4.3.1 τ close to i

The first one is an example of model (3), where τ is rather close to i . For the numerical values of parameters resulting from the fit, we obtain in this case:

$$\begin{aligned} \frac{a_D}{d_D} &= -9.38 \times 10^{-4}, & \frac{b_D}{d_D} &= -1.83 \times 10^{-2}, & \frac{c_D}{d_D} &= 2.66 \times 10^{-5}, & \frac{e_D}{d_D} &= 7.65 \times 10^{-3}, \\ \frac{f_D}{d_D} &= 3.58 \times 10^{-6}, & \frac{a_U}{d_U} &= 5.39 \times 10^{-6}, & \frac{b_U}{d_U} &= 2.80 \times 10^{-3}, & \frac{c_U}{d_U} &= 0, & \frac{e_U}{d_U} &= 0, & \frac{f_U}{d_U} &= 0, \\ g_D &= 1.199, & \tau &= 0.2505 + i 1.1356, & N\sigma &= 0.15. \end{aligned} \quad (45)$$

Both the constants multiplying the modular forms present in M_D and the other constants in M_D and M_U have very different values with the their relevant ratios exhibiting strong hierarchies. The results of the fit of the observables are shown in Table 10.

	$\frac{m_s}{m_b} \times 10^2$	$\frac{m_d}{m_b} \times 10^4$	$\frac{m_c}{m_t} \times 10^3$	$\frac{m_u}{m_t} \times 10^6$	$ V_{us} $	$ V_{cb} $	$ V_{ub} $	$ J_{CP} $	δ_{CP}
Fit	1.87	9.13	2.80	5.39	0.2250	0.0400	0.00353	2.84×10^{-5}	66.5°
Exp	1.82	9.21	2.80	5.39	0.2250	0.0400	0.00353	2.80×10^{-5}	66.2°
1σ	± 0.10	± 1.02	± 0.12	± 1.68	± 0.0007	± 0.0008	± 0.00013	$^{+0.14}_{-0.12} \times 10^{-5}$	$^{+3.4^\circ}_{-3.6^\circ}$

Table 10: Results of the fits of the quark mass ratios, CKM mixing angles, J_{CP} and δ_{CP} . 'Exp' denotes the values of the observables at the GUT scale, including 1σ error.

4.3.2 τ close to ω

We present the second example, in which the VEV of the modulus τ is close to the fixed point ω . The numerical values of parameters obtained in the fit are:

$$\begin{aligned}
\frac{a_D}{d_D} &= 9.68 \times 10^{-4}, & \frac{b_D}{d_D} &= 1.82 \times 10^{-2}, & \frac{c_D}{d_D} &= 4.00 \times 10^{-4}, & \frac{e_D}{d_D} &= -3.04 \times 10^{-2}, \\
\frac{f_D}{d_D} &= -2.65 \times 10^{-6}, & \frac{a_U}{d_U} &= 5.39 \times 10^{-6}, & \frac{b_U}{d_U} &= 2.80 \times 10^{-3}, & \frac{c_U}{d_U} &= 0, & \frac{e_U}{d_U} &= 0, & \frac{f_U}{d_U} &= 0, \\
g_D &= -0.869, & \tau &= -0.4706 + i 0.9359, & \tau - \omega &= 0.0295 + i 0.0699, & N\sigma &= 0.24.
\end{aligned} \tag{46}$$

As in the previous examples, there is a strong hierarchy among both the constants multiplying the modular forms present in M_D and the other constants in M_D and M_U .

The results of the fit of the observables are shown in Table 11.

	$\frac{m_s}{m_b} \times 10^2$	$\frac{m_d}{m_b} \times 10^4$	$\frac{m_c}{m_t} \times 10^3$	$\frac{m_u}{m_t} \times 10^6$	$ V_{us} $	$ V_{cb} $	$ V_{ub} $	$ J_{CP} $	δ_{CP}
Fit	1.86	9.43	2.80	5.39	0.2250	0.0400	0.00354	2.84×10^{-5}	66.4°
Exp	1.82	9.21	2.80	5.39	0.2250	0.0400	0.00353	2.80×10^{-5}	66.2°
1σ	± 0.10	± 1.02	± 0.12	± 1.68	± 0.0007	± 0.0008	± 0.00013	$^{+0.14}_{-0.12} \times 10^{-5}$	$^{+3.4^\circ}_{-3.6^\circ}$

Table 11: Results of the fits of the quark mass ratios, CKM mixing angles, J_{CP} and δ_{CP} . 'Exp' denotes the values of the observables at the GUT scale, including 1σ error.

4.3.3 τ "close" to $i\infty$

Finally, we present an example at the VEV of τ having a relatively large imaginary part "close" to $i\infty$. The numerical values of parameters obtained in the fit are:

$$\begin{aligned} \frac{a_D}{d_D} &= 9.45 \times 10^{-4}, & \frac{b_D}{d_D} &= -1.83 \times 10^{-2}, & \frac{c_D}{d_D} &= -8.22 \times 10^{-6}, & \frac{e_D}{d_D} &= -3.54 \times 10^{-3}, \\ \frac{f_D}{d_D} &= -1.28 \times 10^{-5}, & \frac{a_U}{d_U} &= 5.39 \times 10^{-6}, & \frac{b_U}{d_U} &= 2.80 \times 10^{-3}, & \frac{c_U}{d_U} &= 0, & \frac{e_U}{d_U} &= 0, & \frac{f_U}{d_U} &= 0, \\ g_D &= 0.00925, & \tau &= -0.288076 + i 1.68188, & N\sigma &= 0.097. \end{aligned} \quad (47)$$

In this example, there is also a strong hierarchy among both the constants multiplying the modular forms present in M_D and the other constants in M_D and M_U .

The results of the fit of the observables are shown in Table 12.

	$\frac{m_s}{m_b} \times 10^2$	$\frac{m_d}{m_b} \times 10^4$	$\frac{m_c}{m_t} \times 10^3$	$\frac{m_u}{m_t} \times 10^6$	$ V_{us} $	$ V_{cb} $	$ V_{ub} $	$ J_{CP} $	δ_{CP}
Fit	1.87	9.24	2.80	5.39	0.2250	0.0400	0.00352	2.83×10^{-5}	66.4°
Exp	1.82	9.21	2.80	5.39	0.2250	0.0400	0.00353	2.80×10^{-5}	66.2°
1σ	± 0.10	± 1.02	± 0.12	± 1.68	± 0.0007	± 0.0008	± 0.00013	$^{+0.14}_{-0.12} \times 10^{-5}$	$^{+3.4^\circ}_{-3.6^\circ}$

Table 12: Results of the fits of the quark mass ratios, CKM mixing angles, J_{CP} and δ_{CP} . 'Exp' denotes the values of the observables at the GUT scale, including 1σ error.

5 A texture realizing modulus stabilisation

5.1 Modulus stabilisation

We have performed statistical analyses of the three models and have shown that they are phenomenologically viable. We have shown that model (1) (Eq. (12)), model (2) (Eq. (19) and model (3) (Eq. (23) and the related discussion) can describe well the quark data for values of τ_{VEV} close to i , τ_{VEV} close to $\omega = -0.5 + i\sqrt{3}/2$ (the left cusp) and τ_{VEV} "close" to $i\infty$. The values of the VEV of the modulus τ , $\tau_{VEV} = i$, $\tau_{VEV} = \omega$ and $\tau_{VEV} = i\infty$, as is well known, are the only fixed points of the modular group in its fundamental domain. Values of τ_{VEV} close to three fixed points have been found in studies of the modulus stabilisation (see, e.g., [70–78]), in which τ_{VEV} is obtained by analysing the absolute minima of relatively simple (supergravity-motivated) modular- and CP-invariant potentials for the modulus τ . In this section, we focus on the solution, which give the absolute minima of the supergravity-motivated modular- and CP-invariant potentials for the modulus τ , obtained in Ref. [73]. The values of τ_{VEV} are very close to the fixed point ω for the non-negative integer (m, n) , which denote the power indices in the modular-invariant function, as seen in Table 13.

	τ_{VEV}
$n = 0, m = 1$	$-0.484 + 0.884 i$
$n = 0, m = 2$	$-0.492 + 0.875 i$
$n = 0, m = 3$	$-0.495 + 0.872 i$

Table 13: Values of the modulus τ_{VEV} at the global minima of the the supergravity-motivated modular- and CP-invariant potentials in Ref. [73]. Here, (m, n) denote the power indices in the modular-invariant function.

In the next subsection, we present a model, which is consistent with τ_{VEV} in Table 13.

5.2 An alternative texture zero

In the standpoint of "Occam's Razor approach" of the quark mass matrix (minimum number of parameters) [90], we consider the following texture zeros for mass matrices of the down-type quarks with the diagonal up-type quark mass matrix.

$$M_D = v_D \begin{pmatrix} 0 & 0 & a_D \\ 0 & b_D & c_D \\ d_D & e_D & f_D e^{-i\phi_D} \end{pmatrix}_{RL}, \quad M_U = v_U \begin{pmatrix} a_U & 0 & 0 \\ 0 & b_U & 0 \\ 0 & 0 & d_U \end{pmatrix}_{RL}, \quad (48)$$

where $a_D, b_D, c_D, d_D, e_D, f_D, a_U, b_U, c_U, d_U, e_U$ and f_U are real, and ϕ_D is the CP phase. For down-type quark sector, we obtain those numerical values by inputting observed ones in Appendix B as follows:

$$\begin{aligned} \frac{b_D}{a_D} &= 0.2646, & \frac{c_D}{a_D} &= 7.0815, & \frac{d_D}{a_D} &= 0.05156, & \frac{e_D}{a_D} &= 0.3092, & \frac{f_D}{a_D} &= 5.8735, \\ \varphi_D &= -43.55^\circ, & N\sigma &= 0.0433. \end{aligned} \quad (49)$$

	$\frac{m_s}{m_b} \times 10^2$	$\frac{m_d}{m_b} \times 10^4$	$\frac{m_c}{m_t} \times 10^3$	$\frac{m_u}{m_t} \times 10^6$	$ V_{us} $	$ V_{cb} $	$ V_{ub} $	$ J_{\text{CP}} $	δ_{CP}
Fit	1.87	9.19	*	*	0.2250	0.0400	0.00353	2.83×10^{-5}	66.2°
Exp	1.82	9.21	2.80	5.39	0.2250	0.0400	0.00353	2.8×10^{-5}	66.2°
1σ	± 0.10	± 1.02	± 0.12	± 1.68	± 0.0007	± 0.0008	± 0.00013	$^{+0.14}_{-0.12} \times 10^{-5}$	$^{+3.4^\circ}_{-3.6^\circ}$

Table 14: Results of the fits of the quark mass ratios, CKM mixing angles, J_{CP} and δ_{CP} . 'Exp' denotes the values of the observables at the GUT scale, including 1σ error.

It is emphasized that the numerical values of the parameter set are unique in these mass matrices because the number of parameters is ten while input data are also ten.

5.3 Variant of model (1)

We consider the variant model of the model (1) in Table 1. We show the assignment of the representations and weights for the relevant quarks in Table 15, where the assignments of (u^c, c^c, t^c) are changed:

	$(d, u)_L, (s, c)_L, (b, t)_L$	$(d^c, s^c, b^c), (u^c, c^c, t^c)$	H_U	H_D
$SU(2)$	2	1 1	2	2
A_4	$(1, 1, 1'')$	$(1', 1, 1) (1, 1, 1')$	1	1
k	$(-8, -4, 8)$	$(-8, 4, 8) (8, 4, -8)$	0	0

Table 15: Assignments of A_4 representations and weights.

Since the representations and the weights of the right-handed up-type quarks are different from the down-type ones, the mass matrices are different each other. We have real $\det [M_D] = -a_D b_D d_D$ and $\det [M_U] = a_U b_U d_U$. The mass matrices of the down- and up-type quarks are given as:

$$\begin{aligned}
 M_D &= v_D \begin{pmatrix} 0 & 0 & a_D \\ 0 & b_D & c_Q (2\text{Im}\tau)^6 Y_{1'}^{(12)} \\ d_D & e_D (2\text{Im}\tau)^2 Y_1^{(4)} & f_D (2\text{Im}\tau)^8 (g_D Y_{1'_A}^{(16)} + Y_{1'_B}^{(16)}) \end{pmatrix}_{RL}, \\
 M_U &= v_U \begin{pmatrix} a_U & e_U (2\text{Im}\tau)^2 Y_1^{(4)} & f_U (2\text{Im}\tau)^8 (g_U Y_{1'_A}^{(16)} + Y_{1'_B}^{(16)}) \\ 0 & b_U & c_U (2\text{Im}\tau)^6 Y_{1'}^{(12)} \\ 0 & 0 & d_U \end{pmatrix}_{RL}, \tag{50}
 \end{aligned}$$

In order to reproduce the texture zeros in (48), we choose $c_U = e_U = f_U = 0$ or $c_U, e_U, f_U \ll a_U, b_U, d_U$ by hand.

5.4 Numerical result of the variant model

In the quark mass matrices of Eq.(50), the allowed τ region is obtained by fitting the phase of the texture in (48) with error bar 1% as discussed in section 3. We show the full allowed region in Fig.9 and the restricted region close to the fixed point $\tau = \omega$ in Fig.10.

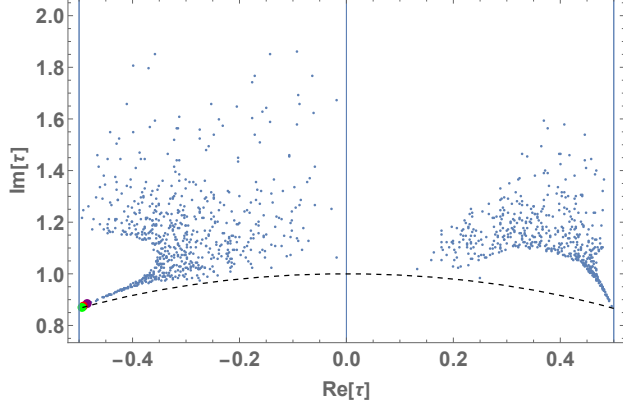


Figure 9: Allowed region in the fundamental domain. Purple, red and green points close to ω denote the τ in the cases of $m = 1, 2, 3$ with $n = 0$, respectively. The dotted curves denotes the boundary of $|\tau| = 1$.

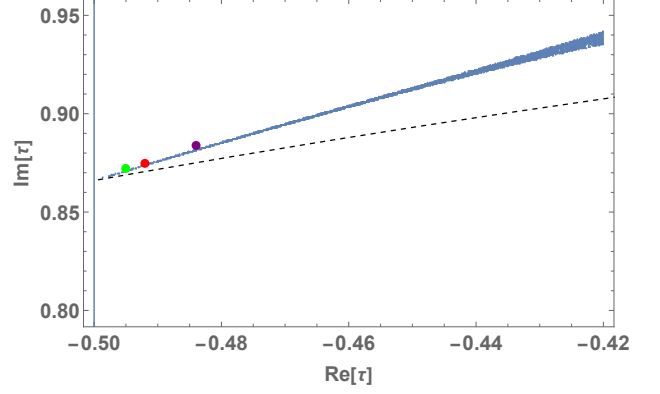


Figure 10: Allowed region close to ω . Purple, red and green points denote the τ in the cases of $m = 1, 2, 3$ with $n = 0$, respectively. The dotted curves denotes the boundary of $|\tau| = 1$.

It is remarked that the three points in Table 13 are almost on the line, which is very narrow allowed region. These three points are never inside the allowed region in the previous models as seen in Figs.1, 3, 5, 7.

Indeed, we obtain a successful example fitting quark masses and CKM parameters by fixing $\tau = -0.492 + 0.875i$, which corresponds to $(m.n) = (2, 0)$ in Table 13 as follows:

$$\begin{aligned} \frac{b_D}{a_D} = 0.2717, \quad \frac{c_D}{a_D} = -78.09, \quad \frac{d_D}{a_D} = 0.05323, \quad \frac{e_D}{a_D} = -1.431, \quad \frac{f_D}{a_D} = 0.01308, \\ g_D = -1.490, \quad \tau = -0.492 + 0.875i, \quad N\sigma = 0.861, \end{aligned} \quad (51)$$

where the up-type quark mass matrix is diagonal. The output is given in Table 16.

	$\frac{m_s}{m_b} \times 10^2$	$\frac{m_d}{m_b} \times 10^4$	$\frac{m_c}{m_t} \times 10^3$	$\frac{m_u}{m_t} \times 10^6$	$ V_{us} $	$ V_{cb} $	$ V_{ub} $	$ J_{CP} $	δ_{CP}
Fit	1.94	9.11	*	*	0.2250	0.0398	0.00354	2.85×10^{-5}	67.6°
Exp	1.82	9.21	2.80	5.39	0.2250	0.0400	0.00353	2.8×10^{-5}	66.2°
1σ	± 0.10	± 1.02	± 0.12	± 1.68	± 0.0007	± 0.0008	± 0.00013	$^{+0.14}_{-0.12} \times 10^{-5}$	$^{+3.4^\circ}_{-3.6^\circ}$

Table 16: Results of the fits of the quark mass ratios, CKM mixing angles, J_{CP} and δ_{CP} . 'Exp' denotes the values of the observables at the GUT scale, including 1σ error.

6 Summary and discussions

We have discussed the strong CP problem within the modular invariance approach to flavour. Working with A_4 ($N = 3$) modular symmetry we have constructed simple models which provide solution to the strong CP problem without the need for an axion. In these models it is assumed that CP is a fundamental symmetry of the Lagrangian. As a consequence, the strong CPV phase $\bar{\theta} = 0$. The CP symmetry is broken spontaneously by the VEV of the modulus τ (τ_{VEV}), so the large CPV phases in the CKM matrix is generated and at the same time $\bar{\theta}$ remains zero or gets a tiny value compatible with the existing stringent experimental limit $\bar{\theta} < 10^{-10}$.

To be more specific, we have considered three models, i.e., three types of down-type and up-type mass matrices M_D and M_U , which have, as a consequence of the A_4 modular symmetry, three zero elements, or three texture zeros, each (Eqs. (12), (19) and (23)). The position of the zeros and the requirement of CP invariance ensures that $\det M_D$ and $\det M_U$ are real quantities. The quark mass matrices M_D and M_U contain three A_4 modular forms of weights 12 and 16 which are $\mathbf{1}'$ singlets, $Y_{1'}^{(12)}$, $Y_{1'A}^{(16)}$ and $Y_{1'B}^{(16)}$, and one modular form of weight 4 which is $\mathbf{1}$ singlet, $Y_1^{(4)}$. The presence of two modular forms of the same weight furnishing the same singlet representation of A_4 is required in order to describe correctly the observed CP violation in the quark sector when the CP symmetry is broken spontaneously by τ_{VEV} . In the case of model (3) we have considered phenomenologically the presence of three additional zero elements in M_U to reduce the number of redundant constant parameters in the model. This set-up, in which M_U is a diagonal matrix, is not guaranteed by modular invariance without additional (symmetry) assumptions.

Our work is an extension of the pioneering work of Ref. [29] where one pattern of texture zeros is considered in the framework of the level $N = 1$ modular symmetry. We have presented phenomenologically viable models with finite modular symmetry of level $N = 3$ (A_4) by using three patterns of texture zeros. We have studied the distributions of the VEV of the modulus τ allowing to reproduce the observed quark masses CKM mixing angles and CP violation. And we have found examples of the models which are viable for values of τ_{VEV} close to the fixed points of the modular group.

In particular, we focus on the VEV of τ , which gives the absolute minima of the supergravity-motivated modular- and CP-invariant potentials for the modulus τ , so called, modulus stabilisation [73]. We present a successful model, which is consistent with this results of the modulus stabilisation.

Our work together with Ref. [29] promotes the modular invariance as a successful approach and framework providing solutions not only to the quark and lepton flavour problems but also to the strong CP problem.

Acknowledgments

The work of S. T. P. was supported in part by the European Union's Horizon 2020 research and innovation programme under the Marie Skłodowska-Curie grant agreement No. 860881-HIDDeN, by the Italian INFN program on Theoretical Astroparticle Physics and by the World Premier International Research Center Initiative (WPI Initiative, MEXT), Japan. The authors would like to thank Kavli IPMU, University of Tokyo, where part of this study was done, for the kind hospitality.

Appendix

A Modular forms of A_4 with higher weights

The lowest weight 2 triplet modular forms of A_4 are given as:

$$\mathbf{Y}_3^{(2)} = \begin{pmatrix} Y_1 \\ Y_2 \\ Y_3 \end{pmatrix} = \begin{pmatrix} 1 + 12q + 36q^2 + 12q^3 + \dots \\ -6q^{1/3}(1 + 7q + 8q^2 + \dots) \\ -18q^{2/3}(1 + 2q + 5q^2 + \dots) \end{pmatrix}, \quad (52)$$

where $q = \exp[2\pi i\tau]$. They satisfy also the constraint [25]:

$$Y_2^2 + 2Y_1Y_3 = 0. \quad (53)$$

For weight 4, five modular forms are given as:

$$\mathbf{Y}_1^{(4)} = Y_1^2 + 2Y_2Y_3 = E_4, \quad \mathbf{Y}_{1'}^{(4)} = Y_3^2 + 2Y_1Y_2, \quad \mathbf{Y}_{1''}^{(4)} = 0,$$

$$\mathbf{Y}_3^{(4)} = \begin{pmatrix} Y_1^{(4)} \\ Y_2^{(4)} \\ Y_3^{(4)} \end{pmatrix} = \begin{pmatrix} Y_1^2 - Y_2Y_3 \\ Y_3^2 - Y_1Y_2 \\ Y_2^2 - Y_1Y_3 \end{pmatrix}, \quad (54)$$

where $\mathbf{Y}_{1''}^{(4)}$ vanishes due to the constraint of Eq. (53).

For weigh 6, there are seven modular forms as:

$$\mathbf{Y}_1^{(6)} = Y_1^3 + Y_2^3 + Y_3^3 - 3Y_1Y_2Y_3 = E_6,$$

$$\mathbf{Y}_3^{(6)} \equiv \begin{pmatrix} Y_1^{(6)} \\ Y_2^{(6)} \\ Y_3^{(6)} \end{pmatrix} = (Y_1^2 + 2Y_2Y_3) \begin{pmatrix} Y_1 \\ Y_2 \\ Y_3 \end{pmatrix}, \quad \mathbf{Y}_{3'}^{(6)} \equiv \begin{pmatrix} Y_1'^{(6)} \\ Y_2'^{(6)} \\ Y_3'^{(6)} \end{pmatrix} = (Y_3^2 + 2Y_1Y_2) \begin{pmatrix} Y_3 \\ Y_1 \\ Y_2 \end{pmatrix}. \quad (55)$$

For weigh 8, there are nine modular forms as:

$$\begin{aligned} \mathbf{Y}_1^{(8)} &= (Y_1^2 + 2Y_2Y_3)^2 = E_8 = E_4^2, & \mathbf{Y}_{1'}^{(8)} &= (Y_1^2 + 2Y_2Y_3)(Y_3^2 + 2Y_1Y_2), & \mathbf{Y}_{1''}^{(8)} &= (Y_3^2 + 2Y_1Y_2)^2, \\ \mathbf{Y}_3^{(8)} &\equiv \begin{pmatrix} Y_1^{(8)} \\ Y_2^{(8)} \\ Y_3^{(8)} \end{pmatrix} = (Y_1^2 + 2Y_2Y_3) \begin{pmatrix} Y_1^2 - Y_2Y_3 \\ Y_3^2 - Y_1Y_2 \\ Y_2^2 - Y_1Y_3 \end{pmatrix}, & \mathbf{Y}_{3'}^{(8)} &\equiv \begin{pmatrix} Y_1'^{(8)} \\ Y_2'^{(8)} \\ Y_3'^{(8)} \end{pmatrix} = (Y_3^2 + 2Y_1Y_2) \begin{pmatrix} Y_2^2 - Y_1Y_3 \\ Y_1^2 - Y_2Y_3 \\ Y_3^2 - Y_1Y_2 \end{pmatrix}. \end{aligned} \quad (56)$$

For weigh 10, there are eleven modular forms as:

$$\begin{aligned} \mathbf{Y}_1^{(10)} &= (Y_1^2 + 2Y_2Y_3)(Y_1^3 + Y_2^3 + Y_3^3 - 3Y_1Y_2Y_3) = E_{10} = E_4E_6, \\ \mathbf{Y}_{1'}^{(10)} &= (Y_3^2 + 2Y_1Y_2)(Y_1^3 + Y_2^3 + Y_3^3 - 3Y_1Y_2Y_3), \\ \mathbf{Y}_{3,1}^{(10)} &\equiv \begin{pmatrix} Y_{1,1}^{(10)} \\ Y_{2,1}^{(10)} \\ Y_{3,1}^{(10)} \end{pmatrix} = (Y_1^2 + 2Y_2Y_3)^2 \begin{pmatrix} Y_1 \\ Y_2 \\ Y_3 \end{pmatrix}, \\ \mathbf{Y}_{3,2}^{(10)} &\equiv \begin{pmatrix} Y_{1,2}^{(10)} \\ Y_{2,2}^{(10)} \\ Y_{3,2}^{(10)} \end{pmatrix} = (Y_3^2 + 2Y_1Y_2)^2 \begin{pmatrix} Y_2 \\ Y_3 \\ Y_1 \end{pmatrix}, \\ \mathbf{Y}_{3,3}^{(10)} &\equiv \begin{pmatrix} Y_{1,3}^{(10)} \\ Y_{2,3}^{(10)} \\ Y_{3,3}^{(10)} \end{pmatrix} = (Y_1^2 + 2Y_2Y_3)(Y_3^2 + 2Y_1Y_2) \begin{pmatrix} Y_3 \\ Y_1 \\ Y_2 \end{pmatrix}. \end{aligned} \quad (57)$$

For weigh 12, there are thirteen modular forms as:

$$\begin{aligned} \mathbf{Y}_{1A}^{(12)} &= (Y_1^2 + 2Y_2Y_3)^3 = E_4^3, & \mathbf{Y}_{1B}^{(12)} &= (Y_3^2 + 2Y_1Y_2)^3 = E_6^2 - E_4^3, \\ \mathbf{Y}_{1'}^{(12)} &= (Y_1^2 + 2Y_2Y_3)^2(Y_3^2 + 2Y_1Y_2), & \mathbf{Y}_{1''}^{(12)} &= (Y_1^2 + 2Y_2Y_3)(Y_3^2 + 2Y_1Y_2)^2, \\ \mathbf{Y}_3^{(12)} &\equiv \begin{pmatrix} Y_1^{(12)} \\ Y_2^{(12)} \\ Y_3^{(12)} \end{pmatrix} = 2(Y_1^2 + 2Y_2Y_3)^2 \begin{pmatrix} Y_1^2 - Y_2Y_3 \\ Y_3^2 - Y_1Y_2 \\ Y_2^2 - Y_1Y_3 \end{pmatrix}, \\ \mathbf{Y}_{3'}^{(12)} &\equiv \begin{pmatrix} Y_1'^{(12)} \\ Y_2'^{(12)} \\ Y_3'^{(12)} \end{pmatrix} = -2(Y_3^2 + 2Y_1Y_2)^2 \begin{pmatrix} Y_3^2 - Y_1Y_2 \\ Y_2^2 - Y_1Y_3 \\ Y_1^2 - Y_2Y_3 \end{pmatrix}, \\ \mathbf{Y}_{3''}^{(12)} &\equiv \begin{pmatrix} Y_1''^{(12)} \\ Y_2''^{(12)} \\ Y_3''^{(12)} \end{pmatrix} = (Y_1^2 + 2Y_2Y_3)(Y_3^2 + 2Y_1Y_2) \begin{pmatrix} Y_2^2 - Y_1Y_3 \\ Y_1^2 - Y_2Y_3 \\ Y_3^2 - Y_1Y_2 \end{pmatrix}. \end{aligned} \quad (58)$$

For weigh 14, there are fifteen modular forms as:

$$\begin{aligned}
\mathbf{Y}_1^{(14)} &= (Y_1^2 + 2Y_2Y_3)^2(Y_1^3 + Y_2^3 + Y_3^3 - 3Y_1Y_2Y_3) = E_4^2E_6, \\
\mathbf{Y}_{1'}^{(14)} &= (Y_1^2 + 2Y_2Y_3)(Y_3^2 + 2Y_1Y_2)(Y_1^3 + Y_2^3 + Y_3^3 - 3Y_1Y_2Y_3), \\
\mathbf{Y}_{1''}^{(14)} &= (Y_3^2 + 2Y_1Y_2)^2(Y_1^3 + Y_2^3 + Y_3^3 - 3Y_1Y_2Y_3).
\end{aligned} \tag{59}$$

Four triplets are obtained by $\mathbf{Y}_3^{(10)} \otimes \mathbf{Y}_1^{(4)}$ and $\mathbf{Y}_3^{(8)} \otimes \mathbf{Y}_1^{(6)}$.

For weigh 16, there are seventeen modular forms as:

$$\begin{aligned}
\mathbf{Y}_{1A}^{(16)} &= (Y_1^2 + 2Y_2Y_3)^4 = E_4^4, & \mathbf{Y}_{1B}^{(16)} &= (Y_1^2 + 2Y_2Y_3)(Y_3^2 + 2Y_1Y_2)^3 = E_4(E_6^2 - E_4^3), \\
\mathbf{Y}_{1'A}^{(16)} &= (Y_1^2 + 2Y_2Y_3)^3(Y_3^2 + 2Y_1Y_2), & \mathbf{Y}_{1'B}^{(16)} &= (Y_3^2 + 2Y_1Y_2)^4, \\
\mathbf{Y}_{1''}^{(16)} &= (Y_1^2 + 2Y_2Y_3)^2(Y_3^2 + 2Y_1Y_2)^2.
\end{aligned} \tag{60}$$

Four triplets are obtained by $\mathbf{Y}_3^{(12)} \otimes \mathbf{Y}_1^{(4)}$ and $\mathbf{Y}_3^{(10)} \otimes \mathbf{Y}_1^{(6)}$.

The modular form E_k is the holomorphic normalized Eisenstein series with weight k , which is given

$$E_k(\tau) = \frac{1}{2\zeta(k)} \sum_{(m,n) \neq (0,0)} \frac{1}{(m+n\tau)^k}, \tag{61}$$

where m and n are integers.

We show the values of singlets of modular form at the fixed points, i , ω , $i\infty$ in Table 17.

k	\mathbf{r}	$\tau_0 = i$	$\tau_0 = \omega$	$\tau_0 = i\infty$
2	$\mathbf{3}(Y_1, Y_2, Y_3)$	$Y_0(1, 1 - \sqrt{3}, -2 + \sqrt{3})$	$Y_0(1, \omega, -\frac{1}{2}\omega^2)$	$Y_0^2(1, 0, 0)$
4	$\{\mathbf{1}, \mathbf{1}'\}$	$Y_0^2\{(6\sqrt{3} - 9), -(6\sqrt{3} - 9)\}$	$Y_0^2(0, \frac{9}{4}\omega)$	$Y_0^2\{1, 0\}$
6	$\mathbf{1}$	0	$Y_0^3 \frac{27}{8}$	Y_0^3
8	$\mathbf{1}$	$Y_0^4 27(7 - 4\sqrt{3})$	0	Y_0^4
	$\mathbf{1}'$	$-Y_0^4 27(7 - 4\sqrt{3})$	0	0
	$\mathbf{1}''$	$Y_0^4 27(7 - 4\sqrt{3})$	$Y_0^4 \frac{81}{16}\omega^2$	0
10	$\{\mathbf{1}, \mathbf{1}'\}$	$Y_0^5\{0, 0\}$	$Y_0^5(0, \frac{243}{32}\omega)$	$Y_0^5\{1, 0\}$
12	$\{\mathbf{1}_A, \mathbf{1}_B\}$	$81Y_0^6\{(26\sqrt{3} - 45), -(26\sqrt{3} - 45)\}$	$Y_0^6\{0, \frac{729}{64}\}$	$Y_0^6\{1, 0\}$
	$\{\mathbf{1}', \mathbf{1}''\}$	$-81Y_0^6\{(26\sqrt{3} - 45), -(26\sqrt{3} - 45)\}$	$\{0, 0\}$	$\{0, 0\}$
14	$\{\mathbf{1}, \mathbf{1}', \mathbf{1}''\}$	$\{0, 0, 0\}$	$Y_0^7\{0, 0, \frac{2187}{128}\omega^2\}$	$Y_0^7\{1, 0, 0\}$
16	$\{\mathbf{1}_A, \mathbf{1}_B\}$	$729Y_0^8\{-(56\sqrt{3} - 97), (56\sqrt{3} - 97)\}$	$\{0, 0\}$	$Y_0^8(1, 0)$
	$\{\mathbf{1}'_A, \mathbf{1}'_B\}$	$729Y_0^8\{(56\sqrt{3} - 97), -(56\sqrt{3} - 97)\}$	$Y_0^8\{0, \frac{6561}{256}\omega\}$	$\{0, 0\}$
	$\mathbf{1}''$	$-729Y_0^8(56\sqrt{3} - 97)$	0	0
	$Y_0 = Y_1(\tau_0)$	$Y_1(i) = 1.0225\dots$	$Y_1(\omega) = 0.948\dots$	$Y_1(i\infty) = 1$

Table 17: Modular forms of singlets with weight $k = 4, 6, 8, 10, 12, 14, 16$, at the fixed point τ_0 .

B Input data of quark masses and CKM elements

The modulus τ breaks the modular invariance by obtaining a VEV at some high mass scale. We assume this to be the GUT scale. Correspondingly, the values of the quark masses and CKM parameters at the GUT scale play the role of the observables that have to be reproduced by the considered quark flavour models. They are obtained using the renormalisation group (RG) equations which describe the “running” of the observables of interest from the electroweak scale, where they are measured, to the GUT scale. In the analyses which follow we adopt the numerical values of the quark Yukawa couplings at the GUT scale 2×10^{16} GeV derived in the framework of the minimal SUSY breaking scenarios with $\tan \beta = 5$ [79]:

$$\begin{aligned}
\frac{y_d}{y_b} &= 9.21 \times 10^{-4} (1 \pm 0.111), & \frac{y_s}{y_b} &= 1.82 \times 10^{-2} (1 \pm 0.055), \\
\frac{y_u}{y_t} &= 5.39 \times 10^{-6} (1 \pm 0.311), & \frac{y_c}{y_t} &= 2.80 \times 10^{-3} (1 \pm 0.043).
\end{aligned} \tag{62}$$

The quark masses are given as $m_q = y_q v_H$ with $v_H = 174$ GeV. The choice of relatively small value of $\tan \beta$ allows us to avoid relatively large $\tan \beta$ -enhanced threshold corrections in the RG running of the Yukawa couplings. We set these corrections to zero.

The quark flavour mixing is given by the CKM matrix, which has three independent mixing angles and one CP violating phase. These mixing angles are given by the absolute values of the three CKM elements $|V_{us}|$, $|V_{cb}|$ and $|V_{ub}|$. We take the present data on the three CKM elements in Particle Data Group (PDG) edition of Review of Particle Physics [7] as:

$$|V_{us}| = 0.22500 \pm 0.00067, \quad |V_{cb}| = 0.04182_{-0.00074}^{+0.00085}, \quad |V_{ub}| = 0.00369 \pm 0.00011. \quad (63)$$

By using these values as input and $\tan \beta = 5$ we obtain the CKM mixing angles at the GUT scale of 2×10^{16} GeV [79]:

$$|V_{us}| = 0.2250 (1 \pm 0.0032), \quad |V_{cb}| = 0.0400 (1 \pm 0.020), \quad |V_{ub}| = 0.00353 (1 \pm 0.036). \quad (64)$$

The tree-level decays of $B \rightarrow D^{(*)}K^{(*)}$ are used as the standard candles of the CP violation. The latest world average of the CP violating phase is given in PDG2022 [7] as:

$$\delta_{CP} = 66.2_{-3.6}^{+3.4} \text{ degrees}. \quad (65)$$

Since the phase is almost independent of the evolution of RG equations, we refer to this value in the numerical discussions. The rephasing invariant CP violating measure J_{CP} [6] is also given in [7]:

$$J_{CP} = 3.08_{-0.13}^{+0.15} \times 10^{-5}. \quad (66)$$

Taking into account the RG effects on the mixing angles for $\tan \beta = 5$, we have at the GUT scale 2×10^{16} GeV:

$$J_{CP} = 2.80_{-0.12}^{+0.14} \times 10^{-5}. \quad (67)$$

C Quark mass matrices with texture zeros

In this Appendix, we present three numerical examples of the quark mass matrix with the texture zeros, which are consistent with the observed masses and CKM elements given in Appendix B.

C.1 Texture (1)

Consider the quark mass matrices with the texture zeros of model (1):

$$M_Q = v_Q \begin{pmatrix} 0 & 0 & a_Q \\ 0 & b_Q & c_Q \\ d_Q & e_Q & f_Q e^{i\varphi_Q} \end{pmatrix}_{RL}, \quad Q = D, U, \quad (68)$$

where $a_D, b_D, c_D, d_D, e_D, f_D, a_U, b_U, c_U, d_U, e_U, f_U$ are real constants, and ϕ_D, ϕ_U are CP violating (CPV) phases. The determinants of the mass matrices M_D and M_U are real and are given in terms of the real parameters a_Q, b_Q and d_D :

$$\det [M_D] = -a_D b_D d_D, \quad \det [M_U] = -a_U b_U d_U. \quad (69)$$

If these mass matrices keep strictly their zero structures and describe correctly the observed CP violation, they are candidates for solving the strong CP problem.

Since the number of parameters in M_D and M_U are 14, four parameters are redundant from the point of view of reproducing the six quark masses and the four independent CKM mixing angles and CPV phase (10 observables). We present the mass matrices in the case of $|a_Q| \sim |b_Q| \sim |d_Q|$. Using as input the observed quark masses and the CKM parameters and performing a statistical analysis we show a typical numerical example of the mass matrices which reproduce the quark data in Appendix B:

$$M_D \sim \begin{pmatrix} 0 & 0 & 1 \\ 0 & 0.901 & -11.63 \\ 0.105 & -0.695 & 12.96 e^{i24.36^\circ} \end{pmatrix}, \quad M_U \sim \begin{pmatrix} 0 & 0 & 1 \\ 0 & 1.23 & -80.80 \\ -0.586 & 9.63 & 386.81 e^{-i150.26} \end{pmatrix}, \quad (70)$$

where $|a_Q| \sim |b_Q| \sim |d_Q|$ are approximately satisfied with only $|d_D|$ being somewhat smaller than the other five constants⁷. The matrices M_D and M_U with the numerical values of the real constants and of the CPV phases $\varphi_D = 24.13^\circ$ and $\varphi_U = -150.26^\circ$ as given in Eq. (70), provide a good quality of the fit of the quark mass ratios, the CKM mixing angles and the CPV phase δ_{CP} ($N\sigma = 0.840$ C.L.), as seen in Table 18.

	$\frac{m_s}{m_b} \times 10^2$	$\frac{m_d}{m_b} \times 10^4$	$\frac{m_c}{m_t} \times 10^3$	$\frac{m_u}{m_t} \times 10^6$	$ V_{us} $	$ V_{cb} $	$ V_{ub} $	$ J_{\text{CP}} $	δ_{CP}
Fit	1.86	9.52	2.80	4.18	0.2249	0.0400	0.00355	2.86×10^{-5}	67.0°
Exp	1.82	9.21	2.80	5.39	0.2250	0.0400	0.00353	2.80×10^{-5}	66.2°
1σ	± 0.10	± 1.02	± 0.12	± 1.68	± 0.0007	± 0.0008	± 0.00013	${}^{+0.14}_{-0.12} \times 10^{-5}$	${}^{+3.4^\circ}_{-3.6^\circ}$

Table 18: Results of the fits of the quark mass ratios, CKM mixing angles, J_{CP} and δ_{CP} . 'Exp' denotes the values of the observables at the GUT scale, including 1σ error.

C.2 Texture (2)

Consider next the quark mass matrices with the texture zeros of model (2):

$$M_Q = v_Q \begin{pmatrix} 0 & 0 & a_Q \\ b_Q & 0 & c_Q \\ e_Q & d_Q & f_Q e^{i\varphi_Q} \end{pmatrix}_{RL}, \quad Q = D, U, \quad (71)$$

where again the constants $a_D, b_D, c_D, d_D, e_D, f_D, a_U, b_U, c_U, d_U, e_U, f_U$ are real, and φ_D, φ_U are CPV phases. The determinants of the mass matrices M_D and M_U are given in terms of a_Q, b_Q, d_Q

⁷The magnitudes of the constants, including c_Q, e_Q and $f_Q, Q = D, U$, which in the modular A_4 model multiply the modular forms present in M_D and M_U , are discussed in section 4.

and real:

$$\det [M_D] = a_D b_D d_D, \quad \det [M_U] = a_U b_U d_U. \quad (72)$$

If these mass matrices keep their zero elements strictly zero and describe the the observed CP violation, they are candidates for solving the strong CP problem.

Performing a statistical analysis we have found a typical numerical example of the mass matrices M_D and M_U which describe the quark data in Appendix B:

$$M_D \sim \begin{pmatrix} 0 & 0 & 1 \\ 0.0610 & 0 & 4.576 \\ 0.0380 & 0.733 & 12.901 e^{i 104.836^\circ} \end{pmatrix}, \quad M_U \sim \begin{pmatrix} 0 & 0 & 1 \\ 0.005752 & 0 & 12.44 \\ 0.00290 & 1.625 & 83.89 e^{i 56.64} \end{pmatrix}. \quad (73)$$

The quark mass ratios and the CKM matrix obtained by diagonalising the matrices M_D and M_U given in Eq. (73) are completely consistent with observed one including the CP violating phase δ_{CP} ($N\sigma = 0.217$ C.L.), as seen in Table 19.

	$\frac{m_s}{m_b} \times 10^2$	$\frac{m_d}{m_b} \times 10^4$	$\frac{m_c}{m_t} \times 10^3$	$\frac{m_u}{m_t} \times 10^6$	$ V_{us} $	$ V_{cb} $	$ V_{ub} $	$ J_{\text{CP}} $	δ_{CP}
Fit	1.87	9.21	2.82	5.43	0.2249	0.0400	0.00352	2.82×10^{-5}	66.3°
Exp	1.82	9.21	2.80	5.39	0.2250	0.0400	0.00353	2.80×10^{-5}	66.2°
1σ	± 0.10	± 1.02	± 0.12	± 1.68	± 0.0007	± 0.0008	± 0.00013	$^{+0.14}_{-0.12} \times 10^{-5}$	$^{+3.4^\circ}_{-3.6^\circ}$

Table 19: Results of the fits of the quark mass ratios, CKM mixing angles, J_{CP} and δ_{CP} . 'Exp' denotes the values of the observables at the GUT scale, including 1σ error.

C.3 Texture (3)

Let us analyse finally the quark mass matrices with the texture zeros of model (3):

$$M_Q = v_Q \begin{pmatrix} a_Q & 0 & 0 \\ c_Q & b_Q & 0 \\ f_Q e^{i\varphi_Q} & e_Q & d_Q \end{pmatrix}_{RL}, \quad Q = D, U, \quad (74)$$

where as in the previous two cases the constants $a_D, b_D, c_D, d_D, e_D, f_D, a_U, b_U, c_U, d_U, e_U, f_U$ are real, and φ_D, φ_U are CPV phases. Also in this case the determinants of the quark mass matrices M_D and M_U are given in terms of real parameters, namely of a_Q, b_Q, d_Q , and are real:

$$\det [M_D] = a_D b_D d_D, \quad \det [M_U] = a_U b_U d_U, \quad (75)$$

As in the previous two cases we note that if the zero elements of these mass matrices remain strictly zero, and the mass matrices describe correctly the observed quark masses, and especially

the quark mixing angles and CP violation in the quark sector, they are a candidate for solving the strong CP problem.

We will present next a typical numerical example of the mass matrices which describe the quark data. Since the number of parameters is 14, four parameters are redundant for reproducing the quark masses and CKM elements (10 observables). In this case, following Ref. [90], we set $c_U = e_Q = f_U = 0$ (also $\varphi_U = 0$). Performing a statistical analysis we get a good description of the quark data in Appendix B with:

$$M_D \sim \begin{pmatrix} 0.000948 & 0 & 0 \\ 0.004209 & 0.01828 & 0 \\ 0.003519 e^{i66.25^\circ} & 0.0400 & 1 \end{pmatrix}, \quad M_U \sim \begin{pmatrix} 5.39 \times 10^{-6} & 0 & 0 \\ 0 & 2.80 \times 10^{-3} & 0 \\ 0 & 0 & 1 \end{pmatrix}. \quad (76)$$

The quark mass ratios, and especially the CKM mixing angles, the J_{CP} factor and the CPV phase δ_{CP} obtained using the numerical matrices given in Eq. (76) are completely consistent with observed one ($N\sigma = 0.113$ C.L.), as seen in Table 20.

	$\frac{m_s}{m_b} \times 10^2$	$\frac{m_d}{m_b} \times 10^4$	$\frac{m_c}{m_t} \times 10^3$	$\frac{m_u}{m_t} \times 10^6$	$ V_{us} $	$ V_{cb} $	$ V_{ub} $	$ J_{CP} $	δ_{CP}
Fit	1.87	9.23	2.80	5.39	0.2250	0.0400	0.00352	2.82×10^{-5}	66.2°
Exp	1.82	9.21	2.80	5.39	0.2250	0.0400	0.00353	2.80×10^{-5}	66.2°
1σ	± 0.10	± 1.02	± 0.12	± 1.68	± 0.0007	± 0.0008	± 0.00013	$^{+0.14}_{-0.12} \times 10^{-5}$	$^{+3.4^\circ}_{-3.6^\circ}$

Table 20: Results of the fits of the quark mass ratios, CKM mixing angles, J_{CP} and δ_{CP} . 'Exp' denotes the values of the observables at the GUT scale, including 1σ error.

References

- [1] A. A. Belavin, A. M. Polyakov, A. S. Schwartz and Y. S. Tyupkin, Phys. Lett. B **59** (1975) 85-87.
- [2] R. Jackiw and C. Rebbi, Phys. Rev. Lett. **37** (1976) 172-175.
- [3] C. G. Callan, Jr., R. F. Dashen and D. J. Gross, Phys. Lett. B **63** (1976) 334-340.
- [4] G. 't Hooft, Phys. Rev. Lett. **37** (1976) 8-11.
- [5] C. Abel, S. Afach, N. J. Ayres, C. A. Baker, G. Ban, G. Bison, K. Bodek, V. Bondar, M. Burghoff and E. Chanel, *et al.* Phys. Rev. Lett. **124** (2020) no.8, 081803 [arXiv:2001.11966 [hep-ex]].
- [6] C. Jarlskog, Phys. Rev. Lett. **55** (1985) 1039.

- [7] R. L. Workman *et al.* [Particle Data Group], PTEP **2022** (2022) 083C01.
- [8] R. D. Peccei and H. R. Quinn, Phys. Rev. Lett. **38** (1977) 1440-1443.
- [9] L. Di Luzio, M. Giannotti, E. Nardi and L. Visinelli, Phys. Rept. **870** (2020) 1-117 [arXiv:2003.01100 [hep-ph]].
- [10] A. E. Nelson, Phys. Lett. B **136** (1984) 387-391.
- [11] S. M. Barr, Phys. Rev. Lett. **53** (1984) 329.
- [12] M. Dine and P. Draper, JHEP **08** (2015) 132 [arXiv:1506.05433 [hep-ph]].
- [13] G. Hiller and M. Schmaltz, Phys. Lett. B **514** (2001) 263-268 [arXiv:hep-ph/0105254 [hep-ph]].
- [14] K. S. Babu and R. N. Mohapatra, Phys. Rev. D **41** (1990) 1286.
- [15] L. Bento, G. C. Branco and P. A. Parada, Phys. Lett. B **267** (1991) 95-99.
- [16] R. Kuchimanchi, Phys. Rev. Lett. **76** (1996) 3486-3489. [arXiv:hep-ph/9511376 [hep-ph]].
- [17] S. M. Barr, D. Chang and G. Senjanovic, Phys. Rev. Lett. **67** (1991) 2765-2768.
- [18] Q. Bonnefoy, L. Hall, C. A. Manzari and C. Scherb, Phys. Rev. Lett. **131** (2023) no.22, 221802 [arXiv:2303.06156 [hep-ph]].
- [19] S. Antusch, M. Holthausen, M. A. Schmidt and M. Spinrath, Nucl. Phys. B **877** (2013) 752-771 [arXiv:1307.0710 [hep-ph]].
- [20] R. Harnik, G. Perez, M. D. Schwartz and Y. Shirman, JHEP **03** (2005) 068 [arXiv:hep-ph/0411132 [hep-ph]].
- [21] C. Cheung, A. L. Fitzpatrick and L. Randall, JHEP **01** (2008) 069 [arXiv:0711.4421 [hep-th]].
- [22] L. Vecchi, JHEP **04** (2017) 149 [arXiv:1412.3805 [hep-ph]].
- [23] Z. G. Berezhiani, R. N. Mohapatra and G. Senjanovic, Phys. Rev. D **47** (1993) 5565-5570 [arXiv:hep-ph/9212318 [hep-ph]].
- [24] A. Valenti and L. Vecchi, JHEP **07** (2021) no.152, 152 [arXiv:2106.09108 [hep-ph]].
- [25] F. Feruglio, in From My Vast Repertoire ...: Guido Altarelli's Legacy, A. Levy, S. Forte, Stefano, and G. Ridolfi, eds., pp.227-266, 2019, arXiv:1706.08749 [hep-ph].
- [26] T. Kobayashi, K. Tanaka and T. H. Tatsuishi, Phys. Rev. D **98** (2018) 016004 [arXiv:1803.10391].

- [27] J. T. Penedo and S. T. Petcov, Nucl. Phys. **B939** (2019) 292 [arXiv:1806.11040].
- [28] P. P. Novichkov, J. T. Penedo, S. T. Petcov and A. V. Titov, JHEP **04** (2019) 174 [arXiv:1812.02158 [hep-ph]].
- [29] F. Feruglio, A. Strumia and A. Titov, JHEP **07** (2023) 027 [arXiv:2305.08908 [hep-ph]].
- [30] J. C. Criado and F. Feruglio, SciPost Phys. **5** (2018) 042 [arXiv:1807.01125 [hep-ph]].
- [31] T. Kobayashi, N. Omoto, Y. Shimizu, K. Takagi, M. Tanimoto and T. H. Tatsuishi, JHEP **1811** (2018) 196 [arXiv:1808.03012 [hep-ph]].
- [32] F. J. de Anda, S. F. King and E. Perdomo, Phys. Rev. D **101** (2020) no.1, 015028 [arXiv:1812.05620 [hep-ph]].
- [33] P. P. Novichkov, S. T. Petcov and M. Tanimoto, Phys. Lett. B **793** (2019) 247 [arXiv:1812.11289 [hep-ph]].
- [34] H. Okada and M. Tanimoto, Phys. Lett. B **791** (2019) 54-61 [arXiv:1812.09677 [hep-ph]].
- [35] G. J. Ding, S. F. King and X. G. Liu, JHEP **1909** (2019) 074 [arXiv:1907.11714 [hep-ph]].
- [36] H. Okada and M. Tanimoto, Eur. Phys. J. C **81** (2021) 52 [arXiv:1905.13421 [hep-ph]].
- [37] H. Okada and M. Tanimoto, Phys. Dark Univ. **40** (2023) 101204 [arXiv:2005.00775 [hep-ph]].
- [38] H. Okada and M. Tanimoto, Phys. Rev. D **103** (2021) 015005 [arXiv:2009.14242 [hep-ph]].
- [39] H. Okada and M. Tanimoto, JHEP **03** (2021) 010 [arXiv:2012.01688 [hep-ph]].
- [40] H. Okada, Y. Shimizu, M. Tanimoto and T. Yoshida, JHEP **07** (2021) 184 [arXiv:2105.14292 [hep-ph]].
- [41] T. Kobayashi, H. Otsuka, M. Tanimoto and K. Yamamoto, Phys. Rev. D **105** (2022) 055022 [arXiv:2112.00493 [hep-ph]].
- [42] T. Kobayashi, H. Otsuka, M. Tanimoto and K. Yamamoto, JHEP **08** (2022) 013 [arXiv:2204.12325 [hep-ph]].
- [43] S. T. Petcov and M. Tanimoto, Eur. Phys. J. C **83** (2023) 579 [arXiv:2212.13336 [hep-ph]].
- [44] S. T. Petcov and M. Tanimoto, JHEP **08** (2023) 086 [arXiv:2306.05730 [hep-ph]].
- [45] P. P. Novichkov, J. T. Penedo, S. T. Petcov and A. V. Titov, JHEP **04** (2019) 005 [arXiv:1811.04933 [hep-ph]].
- [46] X. G. Liu and G. J. Ding, JHEP **08** (2019) 134 [arXiv:1907.01488 [hep-ph]].

- [47] P. P. Novichkov, J. T. Penedo and S. T. Petcov, Nucl. Phys. B **963** (2021) 115301 [arXiv:2006.03058 [hep-ph]].
- [48] C. Y. Yao, X. G. Liu and G. J. Ding, Phys. Rev. D **103** (2021) 095013 [arXiv:2011.03501 [hep-ph]].
- [49] G. J. Ding, F. Feruglio and X. G. Liu, SciPost Phys. **10** (2021) 133 [arXiv:2102.06716 [hep-ph]].
- [50] P. P. Novichkov, J. T. Penedo and S. T. Petcov, JHEP **04** (2021) 206 [arXiv:2102.07488 [hep-ph]].
- [51] G. J. Ding, S. F. King and C. Y. Yao, Phys. Rev. D **104** (2021) 055034 [arXiv:2103.16311 [hep-ph]].
- [52] C. C. Li, X. G. Liu and G. J. Ding, JHEP **10** (2021) 238 [arXiv:2108.02181 [hep-ph]].
- [53] I. de Medeiros Varzielas, M. Levy, J. T. Penedo and S. T. Petcov, JHEP **09** (2023) 196 [arXiv:2307.14410 [hep-ph]].
- [54] G. Altarelli and F. Feruglio, Rev. Mod. Phys. **82** (2010) 2701 [arXiv:1002.0211 [hep-ph]].
- [55] H. Ishimori, T. Kobayashi, H. Ohki, Y. Shimizu, H. Okada and M. Tanimoto, Prog. Theor. Phys. Suppl. **183** (2010) 1 [arXiv:1003.3552 [hep-th]].
- [56] H. Ishimori, T. Kobayashi, H. Ohki, H. Okada, Y. Shimizu and M. Tanimoto, Lect. Notes Phys. **858** (2012) 1, Springer.
- [57] T. Kobayashi, H. Ohki, H. Okada, Y. Shimizu and M. Tanimoto, Lect. Notes Phys. **995** (2022) 1, Springer.
- [58] D. Hernandez and A. Y. Smirnov, Phys. Rev. D **86** (2012) 053014 [arXiv:1204.0445 [hep-ph]].
- [59] S. F. King and C. Luhn, Rept. Prog. Phys. **76** (2013) 056201 [arXiv:1301.1340 [hep-ph]].
- [60] S. F. King, A. Merle, S. Morisi, Y. Shimizu and M. Tanimoto, New J. Phys. **16** (2014) 045018 [arXiv:1402.4271 [hep-ph]].
- [61] M. Tanimoto, AIP Conf. Proc. **1666** (2015) 120002.
- [62] S. F. King, Prog. Part. Nucl. Phys. **94** (2017) 217 [arXiv:1701.04413 [hep-ph]].
- [63] S. T. Petcov, Eur. Phys. J. C **78** (2018) 709 [arXiv:1711.10806 [hep-ph]].
- [64] F. Feruglio and A. Romanino, Rev. Mod. Phys. **93** (2021) no.1, 015007 [arXiv:1912.06028 [hep-ph]].

- [65] T. Kobayashi and M. Tanimoto, [arXiv:2307.03384 [hep-ph]].
- [66] J. R. Ellis and M. K. Gaillard, Nucl. Phys. B **150** (1979) 141.
- [67] I. B. Khriplovich, Phys. Lett. B **173** (1986) 193.
- [68] D. Zhang, Nucl. Phys. B **952** (2020) 114935 [arXiv:1910.07869 [hep-ph]].
- [69] P. P. Novichkov, J. T. Penedo, S. T. Petcov and A. V. Titov, JHEP **07** (2019) 165 [arXiv:1905.11970].
- [70] T. Kobayashi, Y. Shimizu, K. Takagi, M. Tanimoto and T. H. Tatsuishi, Phys. Rev. D **100** (2019) 115045 [erratum: Phys. Rev. D **101** (2020) 039904] [arXiv:1909.05139 [hep-ph]].
- [71] H. Abe, T. Kobayashi, S. Uemura and J. Yamamoto, Phys. Rev. D **102** (2020) 045005 [arXiv:2003.03512 [hep-th]].
- [72] K. Ishiguro, T. Kobayashi and H. Otsuka, JHEP **03** (2021) 161 [arXiv:2011.09154 [hep-ph]].
- [73] P. P. Novichkov, J. T. Penedo and S. T. Petcov, JHEP **03** (2022) 149 [arXiv:2201.02020 [hep-ph]].
- [74] K. Ishiguro, H. Okada and H. Otsuka, JHEP **09** (2022) 072 [arXiv:2206.04313 [hep-ph]].
- [75] V. Knapp-Perez, X. G. Liu, H. P. Nilles, S. Ramos-Sanchez and M. Ratz, Phys. Lett. B **844** (2023) 138106 [arXiv:2304.14437 [hep-th]].
- [76] S. F. King and X. Wang, [arXiv:2310.10369 [hep-ph]].
- [77] T. Kobayashi, K. Nasu, R. Sakuma and Y. Yamada, Phys. Rev. D **108** (2023) 115038 [arXiv:2310.15604 [hep-ph]].
- [78] T. Higaki, J. Kawamura and T. Kobayashi, [arXiv:2402.02071 [hep-ph]].
- [79] S. Antusch and V. Maurer, JHEP **1311** (2013) 115 [arXiv:1306.6879 [hep-ph]].
- [80] S. Weinberg, Trans. New York Acad. Sci. **38** (1977) 185.
- [81] R. Gatto, G. Sartori and M. Tonin, Phys. Lett. B **28** (1968) 128.
- [82] H. Fritzsch, Phys. Lett. B **73** (1978) 317.
- [83] H. Fritzsch, Nucl. Phys. B **155** (1979) 189.
- [84] P. Ramond, R. G. Roberts and G. G. Ross, Nucl. Phys. B **406** (1993) 19 [hep-ph/9303320].
- [85] Z. z. Xing and Z. h. Zhao, Nucl. Phys. B **897** (2015) 302 [arXiv:1501.06346 [hep-ph]].

- [86] H. Fritzsch and Z. z. Xing, Phys. Lett. B **555** (2003) 63-70 [arXiv:hep-ph/0212195 [hep-ph]].
- [87] G. C. Branco, L. Lavoura and F. Mota, Phys. Rev. D **39** (1989) 3443.
- [88] G. C. Branco and J. I. Silva-Marcos, Phys. Lett. B **331** (1994) 390.
- [89] G. C. Branco, D. Emmanuel-Costa and R. Gonzalez Felipe, Phys. Lett. B **477** (2000) 147 [arXiv:hep-ph/9911418 [hep-ph]].
- [90] M. Tanimoto and T. T. Yanagida, PTEP **2016** (2016) 043B03 [arXiv:1601.04459 [hep-ph]].
- [91] K. Harigaya, M. Ibe and T. T. Yanagida, Phys. Rev. D **86** (2012) 013002 [arXiv:1205.2198 [hep-ph]].
- [92] M.-C. Chen, S. Ramos-Sanchez and M. Ratz, Phys. Lett. **B801** (2020) 135153 [arXiv:1909.06910].